



Chair of Drilling and Completion Engineering

Master's Thesis



Design Features of Drill Strings with the  
Power Conductor Lines for Electrodrilling

Arseniy Shcherbakov

June 2022



**AFFIDAVIT**

I declare on oath that I wrote this thesis independently, did not use other than the specified sources and aids, and did not otherwise use any unauthorized aids.

I declare that I have read, understood, and complied with the guidelines of the senate of the Montanuniversität Leoben for "Good Scientific Practice".

Furthermore, I declare that the electronic and printed version of the submitted thesis are identical, both, formally and with regard to content.

Date 21.06.2022

---

Signature Author  
Arseniy Shcherbakov

Arseniy Shcherbakov

Master Thesis 2022

Petroleum Engineering

# Design Features of Drill Strings with the Power Conductor Lines for Electrodrilling

Supervisors: Ass. Prof. Dipl.–Ing. Dr.mont.  
Michael Prohaska-Marchried, Prof. Mikhail  
Gelfgat (Gubkin University)

Co-supervisors: Dr.mont. Petr Víta, Alexander  
Fadeikin (Novobur LLC)

Chair of Drilling and Completion Engineering

*In dedication to my parents*



**MONTANUNIVERSITÄT LEOBEN**  
www.unileoben.ac.at

Arseniy Shcherbakov  
2/2 Akademika Volgina street  
117485 MOSCOW  
RUSSIAN FEDERATION

To the Dean of graduate Studies of the Montanuniversitaet Leoben

---

**Declaration of Approval for the Digital Publication of Scientific Theses**

---

I am aware that the thesis entitled "Design Features of Drill String with the Power Conductor Lines for Electrodrilling" will be subject to a plagiarism assessment and may be stored by Montanuniversität Leoben for an unlimited period of time.

I agree that the University Library of Montanuniversität Leoben may publish the thesis open access in the World Wide Web. For embargoed theses this will be done after the embargo expires.

Note: in case you refuse the open access publication in the World Wide Web, the thesis will only be published in printed form (after a possible embargo has expired) in the University Library (dissertations also in the Austrian National Library).

I hereby agree with the open access publication of my thesis on the World Wide Web:

rslves

ONo

Date 21.06.2022

---

Signature Author

## **Acknowledgements**

I wish to express my sincere gratitude to my supervisor, Prof. Mikhail Gelfgat, for support and involvement in mater's thesis writing and the whole studying period.

I take this opportunity to express gratitude to Dr.mont. Petr Víta and Ass. Prof. Dipl.–Ing. Dr.mont. Prohaska-Marchried for their objective and helpful support.

I would also like to show appreciation to chief technology officer of Novobur LLC Alexander Fadeikin for assistance in the experimental part preparation and entire studying period.

I would like to thank Novobur LLC and Neftekamsk Machinery Plant of Special Equipment LLC members for providing an opportunity to perform the experimental part of the thesis.

Finally, I must express my very profound gratitude to my parents for providing me with unfailing support and continuous encouragement throughout my years of study.

## Abstract

From year to year, the well construction process becomes more challenging, the oil and gas industry requires new technologies or upgrades of existing ones to ensure high efficiency and reliability of the drilling process.

Enhancement in the construction feasibility indicators of deep, branched, complex profile and extended reach drilling wells can be achieved through the promotion of technology developed in the middle of the last century and applied in the oil and gas fields of the USSR – electric bottomhole drilling. This technology combines the benefits of drill string with conductor lines and ideal downhole motor, that is independent of the drilling mud type and has a wide range of revolution rates. The new generation of submersible permanent magnet electric motor (PMM) and the new drill string design with power conductor lines (DPC) will have improved performance capabilities that can potentially eliminate the shortcomings of the previous generation.

The features of DPC operational process for ensuring PMM exploitation will be considered in the master thesis. DPC pressure losses analysis in comparison with conventional drill pipes for rotary drilling with hydraulic downhole motors are demonstrated. Analytical and numerical analysis of power conductors affection on pressure losses in DPC were conducted. To further clarify the conductors affection, plan and methodology of experimental test on Neftekamsk Machinery Plant of Special Equipment are presented. The dynamic analysis of DPC operational process for observing sensible design parts with DYNTUB software and bench test preparation are proposed.

## Zusammenfassung

Von Jahr zu Jahr wird der Bohrlochbauprozess anspruchsvoller, die Öl- und Gasindustrie benötigt neue Technologien oder Upgrades bestehender Technologien, um eine hohe Effizienz und Zuverlässigkeit des Bohrprozesses zu gewährleisten.

Eine Verbesserung der Machbarkeitsindikatoren für den Bau von tiefen, verzweigten, komplexen Profil- und Bohrungen kann durch die Förderung einer Technologie erreicht werden, die Mitte des letzten Jahrhunderts entwickelt und in den Öl- und Gasfeldern der UdSSR angewendet wurde – elektrisches Grundlochbohren. Diese Technologie kombiniert die Vorteile eines Bohrstrangs mit Schleifleitungen und einem idealen Bohrlochmotor, der unabhängig vom Bohrschlammtyp ist und einen großen Drehzahlbereich aufweist. Die neue Generation von tauchbaren Permanentmagnet-Elektromotoren (PMM) und das neue Bohrstrangdesign mit Stromleitern (DPC) werden verbesserte Leistungsfähigkeiten aufweisen, die möglicherweise die Mängel der vorherigen Generation beseitigen können.

Die Merkmale des DPC-Betriebsprozesses zur Sicherstellung der PMM-Nutzung werden in der Masterarbeit betrachtet. DPC-Druckverlustanalysen im Vergleich zu konventionellen Bohrgestängen zum Drehbohren mit hydraulischen Bohrlochmotoren werden demonstriert. Analytische und numerische Analysen des Einflusses von Stromleitern auf Druckverluste in DPC wurden durchgeführt. Um die Zuneigung des Dirigenten weiter zu verdeutlichen, werden der Plan und die Methodik des experimentellen Tests in der Neftekamsk Machinery Plant of Special Equipment vorgestellt. Die dynamische Analyse des DPC-Betriebsprozesses zur Beobachtung sensibler Konstruktionsteile mit der DYNTUB-Software und die Vorbereitung von Prüfstandstests werden vorgeschlagen.



# Table of Contents

Acknowledgements.....	iii
Abstract.....	v
Zusammenfassung.....	vi
Chapter 1.....	9
Introduction.....	9
1.1 Background and Context.....	9
1.2 Scope and Objectives.....	10
1.3 Achievements.....	10
1.4 Technical Issues.....	11
1.5 Overview of Dissertation.....	11
Chapter 2.....	13
Literature Review.....	13
2.1 The First Design of Drill Pipes for Electrodrilling.....	13
2.2 Electrical Three-line Drill Pipe Design for Electrodrilling.....	14
2.3 Electrodrilling System of 1970.....	15
2.4 Design of Drill Pipes with Two-line Current Lead.....	16
2.5 Disadvantages of the 60-70s Generation Electrodrill Pipes and Tasks for New Design Development.....	18
2.6 New Electrodrill Pipes Design and their Exploitation Features.....	19
2.7 Features of Drilling with Electric Drill.....	22
2.8 Dynamic Loads.....	26
2.9 Buckling in DP.....	33
2.10 Features of DPC Hydraulic Analysis.....	35
2.11 Summary.....	36
Chapter 3.....	38
DPC Analytical Studies.....	38
3.1 Comparative Hydraulic Analysis of DPC and Traditional Drill Pipes.....	38
3.2 DPC Pressure Losses Analysis via OpenFOAM.....	46
3.3 Dynamic Loads Analysis with DYNTUB Software.....	57
3.4 Summary.....	58
Chapter 4.....	60
DPC Experimental Tests.....	60
4.1 Experimental Test of DPC Pressure Drop Estimation.....	60
4.2 DPC Bench Test on Novobur Vibrostand.....	68
Chapter 5.....	71
Conclusion.....	71
5.1 Summary.....	71

---

5.2	Evaluation.....	72
5.3	Future Work .....	72
	References.....	74
	List of Figures.....	77
	List of Tables .....	78
	Nomenclature.....	79
	Abbreviations.....	80

# Chapter 1

## Introduction

### 1.1 Background and Context

Nowadays, drilling process with hydraulic downhole motors is accompanied using conventional drill pipes and MWD with hydraulic communication channel. However, this traditional approach has certain limitations that are as follows: the permissible drill mud flow rate, the abrasion resistance of MWD system at high solid phase content, the downhole motor parameters dependence on the drilling mud type and flow rate. These limitations force drilling engineers to look for new technologies or technological improvements that can increase well construction efficiency and quality.

The further progress of ROP and well construction quality increasing rest on real-time information transferring technologies shoulders. The breakthrough in well construction technology can be achieved via application of electrodrilling complex based on downhole PMM which is powered by DPC.

Electrodrilling technology possesses certain advantages compared with the conventional technology. As examples of these advantages the following points should be mentioned. PMM is not dependent on flow rate and drilling mud density so the full control over motor shaft revolution rate is ensured consequently. In addition, cable lines provide almost unlimited information transfer between the bottomhole and surface. Apart from that, PMM does not create significant hydraulic losses in mud circulation system therefore there is an increased borehole cleaning effect.

However, experience of 70-80s when the shortcomings of electrodrilling technology were observed, among them low reliability of current lead needed for electricity transferring and

significant pressure losses due to central current lead placement in drill string, should be accounted.

The features of new DPC design for PMM application, that have the potential to achieve technical breakthroughs in well construction and eliminate previous generation shortcomings of electrodrilling complex, will be considered in the master thesis

## **1.2 Scope and Objectives**

The master thesis aims to identify features of using DPC in new electrodrilling complex as well as provide a comparison with conventional drill pipes application.

To achieve the aims, the comparative hydraulic calculations for difference identification between PMM application based on DPC and conventional technology (RSS or PDM) based on conventional DP will be performed using Landmark software. Additional pressure losses during DPC application are created mainly by inner cable location in DPC and decreased cross-section of tool joints. Nevertheless, the additional losses can be compensated by the insignificant pressure losses at PMM in some cases. In addition to this, OpenFoam software will be used to assess the mud flow characteristics in DPC. It will allow determining quite precise values of pressure losses in DPC by simulating its cross-section geometry. Moreover, a full-scale test for determining the most accurate values of hydraulic losses in DPC will be conducted with the help of Neftekamsk Machinery Plant of Special Equipment test facilities. Eventually, the hydraulic calculations allow providing some technical recommendations of certain DPC size application in particular well construction scenario.

The task of providing dynamic analysis of the DPC drilling process in DYNTUB software will be also presented in master thesis. It is known, that DP is exposed to different types of dynamic loads, that may harm drill string integrity and operability. The feature of DPC design is the presence of a communication line mounted inside DPC in the first case and the presence of a communication line inside the wall of the DPC in the second one. Due to the mass-center offset and the increased probability of the communication line detachment, the particular interest arises in the first case of line location. Analysis in DYNTYB software will allow providing dynamic loads assessment as well as developing a testing program (specification) for the dynamic bench test, which would bring the electrodrilling technology to natural drilling conditions.

## **1.3 Achievements**

In the master's thesis, theoretical review and analysis of electric drill complex of 60-70s generation were carried out.

Overview of the new DPC design for electric drilling is given. Software products and methods for analyzing the design features of DPC are proposed.

Comparative hydraulic calculation of electrodrill application and traditional methods of well construction was carried out. Numerical simulation of mud flow process in DPC pipe body has been performed in order to clarify the influence of power conductors on pressure losses. The application of DYNTUB program for dynamic loads analysis in DPC is considered.

Test plan and methodology have been proposed in order to estimate pressure losses in DPC at the Neftekamsk Machine-Building Plant of Special Equipment. Application of Novobur LLC vibrostand for dynamic loads analysis in DPC is considered.

## **1.4 Technical Issues**

It has not been possible to conduct analytical and experimental analysis of dynamic loads occurring in DPC due to financial difficulties in Novobur LLC at the moment. DPC tests at Neftekamsk Machinery Plant of Special Equipment (Neftekamsk, Russia) were delayed for the same reason.

## **1.5 Overview of Dissertation**

In the literature review of master's thesis, electric drilling experience in USSR will be presented, as well as disadvantages of previous generation electric drilling complex. Design features of DPC operating conditions are described, and methods for taking into account the features of such pipes are presented in the same chapter. The fourth chapter discusses analytical studies related to hydraulic losses and dynamic loads in DPC. The fifth chapter presents a methodology and test plan of DPC experimental tests at Neftekamsk Machinery Plant of Special Equipment and vibrostand of Novobur LLC.



# Chapter 2

## Literature Review

Throughout the history, development of electrodrilling method was accompanied by field application that shows significant advantages over the conventional method with using PDM or rotary drilling.

There were main three designs of drill pipes for electrodrilling in the 20th century and each of them had certain features related mostly to the size of current lead and reliability of drill pipes elements. The main design features of current lead and drill pipes elements will be described in this chapter as well as pros and cons which were appeared during the field application.

### 2.1 The First Design of Drill Pipes for Electrodrilling

Over the last century, USA, European and Russian experts have been trying to develop electrodrilling technology. The first efficient EDM complex for drilling was developed in the U.S.S.R. between 1937 and 1940 (Gelfgat Y. et al., 2003).

The electrical supply of three-phase motor in the first variant of electrodrilling complex design was provided by cable lines consisting of three-core cable segments with cable terminal box connecting to each other at drill pipe screwing operation.

Outer diameter of the first contact joint of current lead to EDM-12 (electric downhole motor) developed in 1938-1939 was 80 mm. Elements of current lead was exploited in the quite light working conditions since the power of 70 kW were delivered by them at 700 V and 87 amperage, in the meantime the power of 300 kW at 2000 V and 160 amperage were used in 70s generation electrical drilling complex . The first design had several disadvantages: significant diameter of connection, fracture creating in ebonite contact rod body, non-reliable connection in tool joint and complex system of contact connection sealing (Gelfgat Y. et al., 2003).

The further design development was accompanied with searching for material that is used for contact rod and box developing. The rod body was decided to be made of resin. The other several design modernizations were provided at the same time (Gelfgat Y. et al., 2003).

## 2.2 Electrical Three-line Drill Pipe Design for Electrodrilling

Due to the central location of electrical cable, the cross section of drill pipe decreases especially in places where cable sections attaches to the tool joints, full-opening drill pipes with inner upsets were developed, the outer diameter of the electrical cable was reduced up to 43 mm and contact connection was decreased up to 65mm. The electrical three-line drill pipe design and pipe-to-pipe connection were developed (Fomenko F.N., 1974).

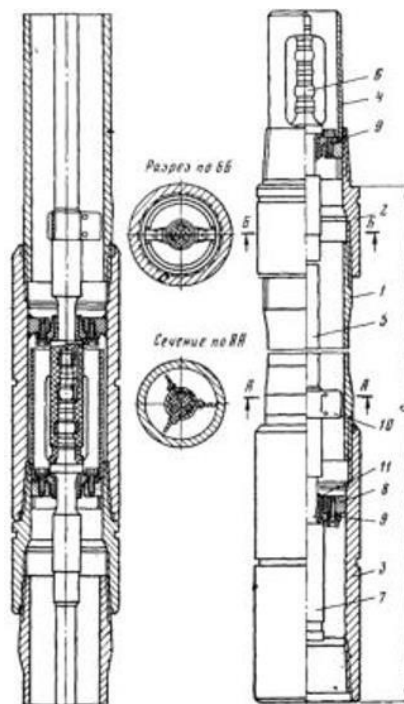


Figure 2.1. Electrical three-line drill pipe design (Fomenko F.N., 1974).

1 – drill pipe body, 2 - tool joint pin, 3 – tool joint box, 4 - connection rod safety tower, 5 - three-core cable, 6 - three-line cable, 7 – three-line box, 8 – tong die, 9 – support, 10 – stabilizer, 11 – protective sleeve.

In 1940 in Kala near Baku village, a well using the new electrodrilling system including electric three-line cable DP was drilled for the first time anywhere in the world. The well was 1500 m deep. Each elements of electrodrilling complex passed this first field test successfully. Based on this test result, the following conclusions were made (Gelfgat Y. et al, 2003):

- Discrete power conductors located in drill pipe could be used to supply EM



- There was significant hydraulic power concentrated at the bit leading to higher ROP in comparison with rotary drilling

Drawbacks connected to drill pipe design revealed during the exploitation period:

- Low reliability of cable section
- Significant pressure losses due to the central current lead location

In order to improve the entire electrodrilling system and electric drill the further theoretical and experimental studies were required. However, due to World War II development of the method was stopped.

Despite low reliability of gearbox, frequent breakdowns of contact between cable sections, increased pressure on pumps, individual elements of the system were continuously improved: downhole equipment, motor design, power cable, connections and auxiliary equipment, because of engineering and scientific research. From 1948 to 1963, motor modifications were developed and commercially applied in former Soviet Union fields. On average, drilling efficiency was 15-20% higher compared to the turbodrill, but the pattern was not observed in all wells (Gelfgat Y. et al., 2003). The lack of a stable positive trend in drilling performance was due to the shortage and remoteness of downhole motor maintenance workshops and need for additional personnel training. During this period, the following shortcomings of the electric drilling technology were identified (Perelman O.M. et al, 2021).

- Low resistance of cable connections and frequent breakdowns of current supply system.
- Significant hydraulic losses, especially in current lead connections and tool joints
- Current lead did not allow auxiliary tool to be run in drill string

These drawbacks were accounted for by experts and companies involved in development of electrodrilling technology.

Due to the design features of DP with three-line cable that create significant hydraulic losses, DP with electrical two-line cable were developed which allowed to supply the three-phase motor via paired (two-line) cable and drill pipes.

### **2.3 Electrodrilling System of 1970**

Based on the previous field experience, electrodrill standard was worked out between 1963 and 1970. There were standards for electrodrills with diameters from 127mm to 240mm as well as auxiliary equipment information (Gelfgat Y et al, 2003). The new commercial electrodrilling complex is presented in fig. 2.2.

The system consisted of the following basic units:

- electrodrill and other parts of the downhole drill string assembly
- telemetric system
- drill pipes with two-line power cable
- automatic bit feed regulator
- transformer for the electrodrill power supply
- control station and board

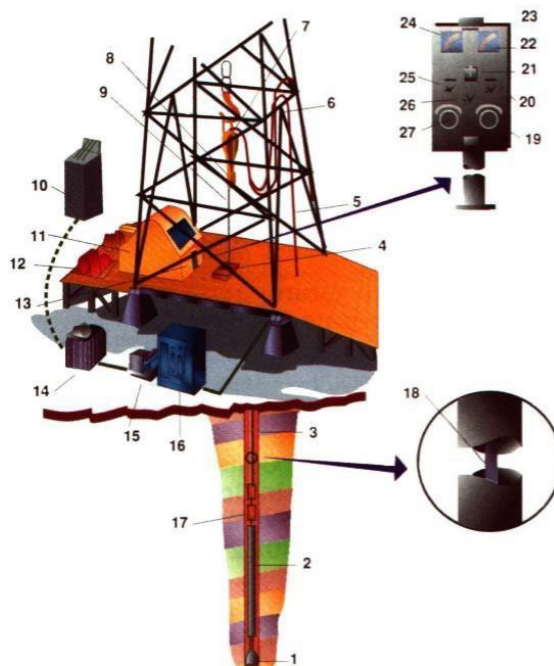


*Figure 2.2. Electrodrilling system of 60-70s generation set-up (Abyzbaev B.I. et al., 2003).*

There was traditional rotary drilling system applied and surface tool (power transformers, current collectors and so on) fabricated as auxiliary tool for basic equipment was used.

## 2.4 Design of Drill Pipes with Two-line Current Lead

The design of drill pipe with two-line current lead and the drill pipe connection is shown on fig.2.3. Two-line cable sections are connected via double contact boxes with diameter of 50mm. The cable has oval cross section with outer diameter of 35x15mm. The third cable is connected to the «ground» with the help of a certain ground connection attached to the drill pipes through current-collecting device, and via immediate contacting with borehole wall and mud (Abyzbaev B.I. et al., 2003).

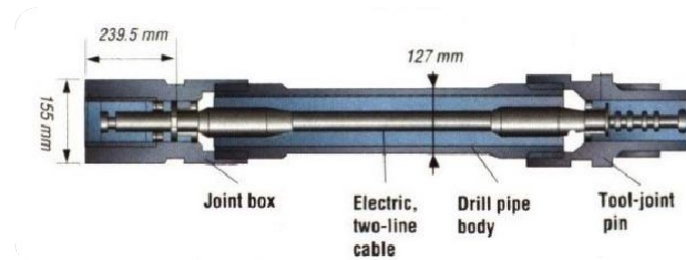


Figure 2.3. Drill pipe with two-line current lead (Abyzbaev B.I. et al., 2003).

When electrodrill supplying using «two-line – drill pipes» system, both cores of two-line cable, three phases of stator coil and power transformer are connected with the «ground» as soon as one phase of stator coil is connected to drill pipe.

Voltage of power transformer secondary coil (energy system) is connected to slip ring brushes of current-collecting devise using a line connector. Cables of two-core current-collecting devise cable are connected to two contacts rings. Voltage supplies to two phases of three-phase motor coil. To supply voltage to the third phase of three-phase motor the drill string is used. The lower end of drill string is connected to the one phase of electrodrill stator coil via submersible contactor (Fomenko F.N.,1968).

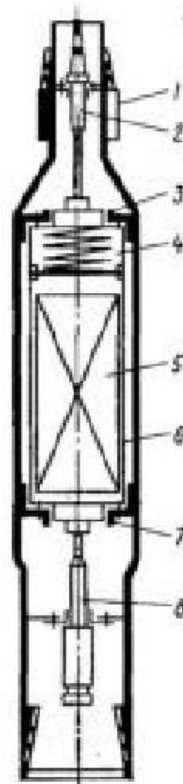


Figure 2.4. Submersible electromagnetic contactor (Fomenko F.N.,1968).

1 – outside case, 2 – double rod of cable-penetration fitting, 3 and 7 - supports, 4 – compensator, 5 –electromagnetic mechanism, 6 – oil-filled container, 8 – three-pin box.

### 2.4.1 Description of the Drill pipes and Tool joints

TBT-114 and TBT-140 with external upsets, and V-127 with inner upsets were applied for electrodrilling. TBT-140 was manufactured with two certain lengths  $11950\pm 50$  and  $12050\pm 50$  mm, TBT-114 had lengths of  $12000\pm 50$  mm.

Thread of drill pipes was manufactured with taper angle of 1:16, tolerance and thread profile were corresponded to GOST-631-63 (Russian standard).

V-127 drill pipes had the same pipe thread as T114. Tool joints for these types of pipe are similar. Tool joints for TBT-140 had bigger length; there was also a presence of a safety bottle in pin part of pipe and a slip segment for cable segment supports attaching as well as a bevel edge on tool box part (Fomenko F.N., 1968).

## 2.5 Disadvantages of the 60-70s Generation Electrodrill Pipes and Tasks for New Design Development

During the field exploitation of 60-70s generation electrodrilling technology drilling efficiency was approximately 15-20% higher compared to turbodrill, but the pattern was not observed in all wells. In addition to that, the following shortcomings of the electric drill pipes were identified.

- Low reliability cable sections connectors for power supply. In the wells of Bashkiria, up to 4 failures were noted per 1200-1700 meters drilled. During drill pipes operational period (15 wells), 10 or more breakdowns were recorded, which led to additional trips for repairs and significant non-productive time. With increasing depth, the situation became even worse - 319 failures associated with cable sections were recorded while drilling well No.157 (4368m) in difficult geological conditions in Azerbaijan. Non-productive time due to trials and repairs exceeded 5000 hours at this well.
- Substantial pressure losses where the current lead passes through the tool joints.
- The inability to run inclinometers on a wireline into the drill string to orient the BHA forced the electric drills to be applied in vertical wells only.

In spite of having the mentioned disadvantages the electrodrilling technology combines the advantages of rotary drilling and drilling with hydraulic downhole motors, but devoid their inherent disadvantages (Perelman O.M. et al., 2021).

For this reason, Novobur LLC started full-scale R&D to develop electrical drilling technology based on permanent magnet submersible electric motor (PMM) with the new design of the electrical drill pipes. These drill pipes allow decreasing the pressure losses and using auxiliary

tools run into the drill string since these pipes have the electrical cable located on the periphery of the inner pipe surface.

To estimate the hydraulic losses of the new electrical drill pipes and the dynamic loads acting on those the special software of DYNTUB and Landmark will be applied. To clarify the value of hydraulic losses experimental test with the use of Neftekamsk Machinery Plant of Special Equipment (NMPSE) testing bench will be performed as well as OpenFOAM simulation. The results of simulation and experiments will allow considering the possible disadvantages of the current DPC design, these will be presented in the next chapters.

## **2.6 New Electrodrill Pipes Design and their Exploitation**

### **Features**

Since 2017, Novobur company, Perm city, has begun full-scale R&D to develop electrical drilling technology based on permanent magnet submersible electric motor (PMM). These motors have been successfully implemented in conjunction with ESP for oil production in dimensions ranging from 80 to 240 mm. Based on modern achievements in the field of material science, special drill pipes are being developed with a concentric Inner placement of electrical cable, as well as coiled tubing with a powered wireline inside.

The main area of new Electrical Drilling Complex (EDC) application is directional drilling of exploration and production wells, complex trajectories, ERD and deep wells. Obviously, EDC significantly differs from conventional approaches, first of all, in the composition of surface equipment: in addition, control station of electrical system is required, a transformer, current lead for supplying power to the drill string, a device for washing the contacts of cable sections before making up connections (Perelman O.M. et al., 2021). Likewise, conventional drill pipes are replaced by pipes with a cable section.

There are two-unit sizes of DPC developed at Novobur LLC: DPC -102 and DPC-127. DPC-102 consist of drill pipe body with cylindrical sleeve installed in the pipe wall and tool joint which is needed for drill pipe connection and electricity transmitting through DPC-102. DPC-127 has other design: the cylindrical sleeve is changed by power conductors located in flow area of DPC-127.

It should be noted, that the key part of the new electrodrilling complex is the drill pipes with power conductors whose electrical boxes are subjected to significant mechanical and electrical loads. To assess operability of the boxes Novobur LLC conducted numerical simulation (Perelman O.M. et al., 2021).

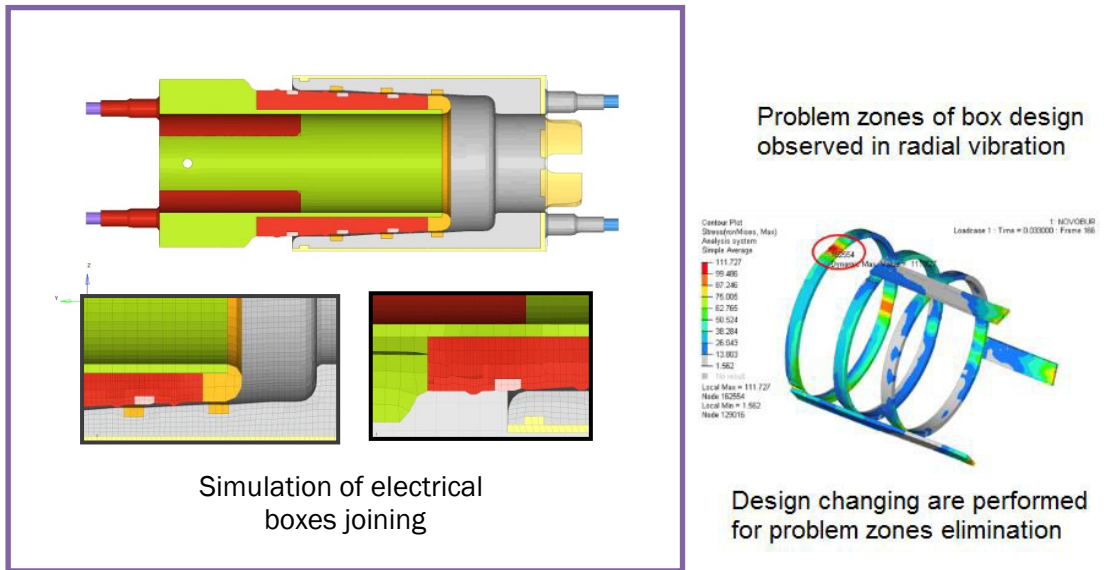
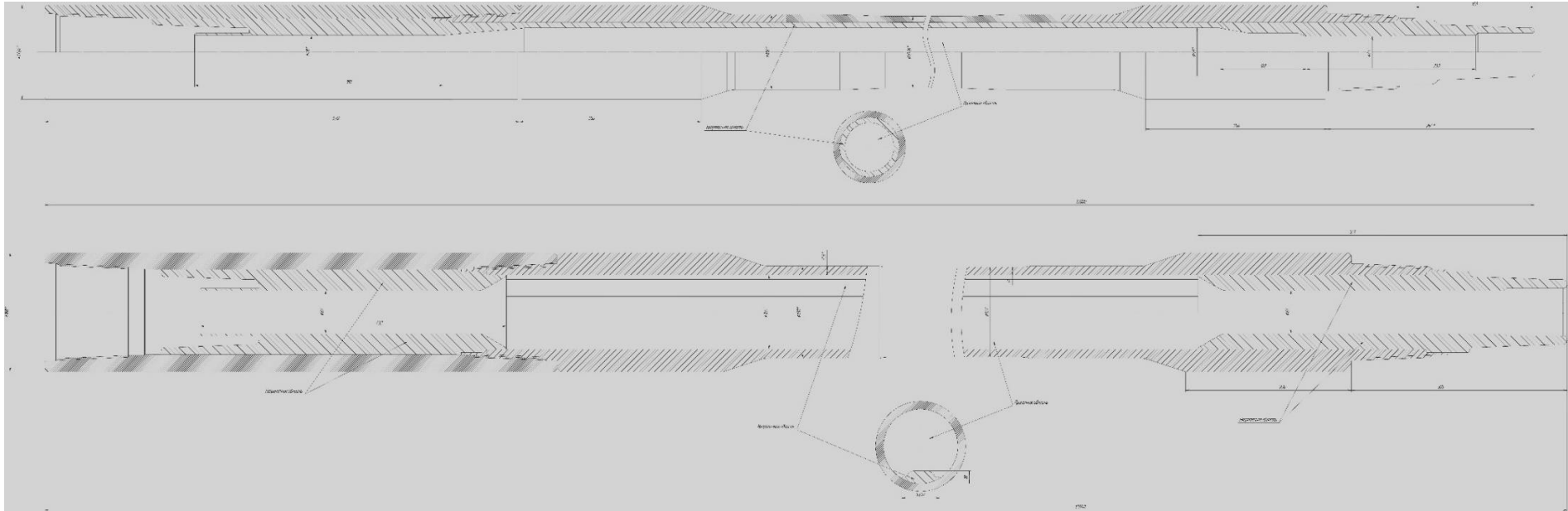


Figure 2.5.R&D conducted by Novobur LLC (Perelman O.M. et al., 2021).



*Figure 2.6.DPC-102 (upper figure) and DPC-127 (lower figure) (Novobur LLC).*

The distinctive feature of new DPC-127 design in comparison with drill pipes with the current lead of the previous generation is power conductors placement on the pipe inner wall. This placement of the power conductors makes it possible to avoid significant pressure losses in the pipes and tool joints, and also allows auxiliary tools to be run into drill string.

DPC differs from standard drill pipes primarily in a reduced flow area in pipe body and tool joint, which requires a comparative analysis of hydraulic program. Power conductor presence inside drill string also poses the task of analyzing dynamic loads that occur in drill string due to center of mass displacement and buckling.

Features and DPC operating conditions, which may affect integrity of its design will be discussed further. The impact of DPC design features on hydraulic losses and dynamic loads will be presented.

## **2.7 Features of Drilling with Electric Drill**

The main features of induction electrodrill of the previous generation as well as new synchronous PMM application will be presented further.

The features of drilling with induction electrodrill are as follows.

1. The electrodrill receives power directly from drilling transformer via cable laid inside drill string. Electricity is transmitted with low losses due to high voltage usage.
2. The electric motor power does not depend on flow rate, drilling mud properties and drilling depth. The feature allows solving the deep wells drilling problem using viscous mud with high density, aerated mud and gaseous agents for borehole cleaning. There is also an opportunity to drill productive intervals with surface active agents being added to mud (Perelman O.M., 2021).
3. The electric drill shaft rotation speed does not depend on amount and drilling mud properties and slightly depends on WOB.
4. The amount of drilling mud during electric drilling is determined mainly by normal hole cleaning conditions, regardless of power developed by the electric drill. Smaller amount of drilling mud is required during electric drilling compared to turbine drilling, where mud circulation rotates turbine.

Reducing the amount of drilling mud contributes to less borehole erosion and reduces caving. In addition, thief zones drilling is possible without complications. Lower pump operating pressure at outlet reduces the requirements for strength of communications hoses, increases service life of pumps, facilitates the operation of pumping unit and drill pipes thread



connections and significantly increases their service life, and also allows to use pressure reserve for jet drill bits (Fomenko F.N. et al, 1974).

5. Direction of drilling mud flow does not affect the electric drill characteristics, which makes it possible to apply reverse mud circulation with small amount of mud and energy consumption for cleaning (Perelman O.M. et al, 2021).

6. Electric drill is sealed oil-filled machine, whose driven elements are not affected by drilling mud abrasive particles. Therefore, characteristics of electric drill does not change throughout its entire service life.

7. Change of bit drag torque during drilling is instantly reflected in change of current and power. It provides with observing bit load using a wattmeter, determine bit operation mode, determine wear severity and prevent bit accidents.

8. Changes in current and power reflecting the load on bit make it possible to automate the drilling process with the best power usage developed by electric drill (Perelman O.M. et al, 2021).

9. Absence of drill string rotation and design features of the electric drill allow using special submersible equipment during directional well drilling to monitor the inclination and azimuth angle, as well as installing of deflecting tool in desired direction and adjust its position after drill pipes descent during bit rotation, taking into account the angle of drill pipes twisting under the electrical drill reactive torque (Fomenko F.N., 1968).

10. When drilling wells with significant value of inclination angle or multilateral horizontal wells, telemetric system can be freely immersed regardless of wellbore inclination and, thus, ensure the measurement of inclination and azimuth angle.

11. Applying of telemetric system over an electric drill makes it possible to adjust the deflecting tool when the drill string is pulled in lateral of multilateral well.

Techniques and technology of electrodrilling are continuously being improved. The features of electrodrilling determine the drilling mode parameters: bit speed, WOB and amount of drilling mud.

Drilling with the electric drill is carried out at almost constant bit speed; speed characteristic of the electric drill is rigid.

Number of pumps, diameter of pump barrel and number of piston strokes are set based on rational well cleaning requirements, regardless of the electrical drill. To increase ROP, it is possible to change WOB only, which directly affects the electric drill loading. This effect varies depending on properties of rock being drilled.

In order to achieve the best drilling performance, it is advisable to drill at high WOB, which directly determines the electric drill loading in terms of power. Permissible electric drill loading depends on permissible heating of motor winding. This loading will coincide with the electro drill rated power if at a given well depth the ambient temperature is equal to design temperature adopted when designing the motor. Taking into account actual thermal conditions of drilling in each specific area, it is worth introducing adjustments into the operating modes of electric drills aimed at increasing electric drill loading in excess of the rated power. Therefore, the temperature of mud circulating should be specified in each new area (Fomenko F.N.,1974).

The exploitation features on the new PMM are as follows (*Perelman O.M. et al., 2021*).

1. Permanent magnet motors without a gearbox at 300 rpm provides approximately the same torque as an induction motor with a gearbox;
2. With the same value of output torque, the length of the active part of the PMM motor is 2 times shorter than induction has, which is essential factor when drilling inclined and horizontal wells;
3. PMM is capable of providing a smooth 3-fold change in the shaft rotational speed during one run, for example, in the range from 100 to 300 rpm, with a constant torque on the motor's shaft;
4. The use of PMM with a gearbox will provide an operating speed range from 30 to 100 rpm, the magnitude of torque will be limited only by strength characteristics of shaft and gearbox.

### **2.7.1 Drilling Modes**

Drilling modes should be selected on basis of data obtained during offset wells drilling and other wells previously drilled in this area.

The electric drill should be turned on (without pulling it in to bottom) after the mud circulation is in stable state. The bottomhole should be reached smoothly with reaming. Then bit breaking-in follows at WOB of 2-5 tons for 2 minutes and bring WOB smoothly to optimum within 5-10 minutes. It is recommended to set and control the bit operating mode by wattmeter and drillometer. According to ammeter readings, maximum permissible value of total current consumed by the electric drill is controlled only. It is not recommended to use ammeter to set the drilling mode, since the total current does not reflect actual power on the electric drill shaft. It is recommended to drill with the electric drill with simultaneous rotation of drill string at speed of 5 - 30 RPM, in geological conditions that cause drill string drag (Fomenko F.N., 1974).

It is recommended to reduce WOB as bit bearing backlash increases for better roller cone bits run. The moment when WOB must be decreased is determined by sharp increase in power recorded by wattmeter. The moment of bit pulling out should be determined by two signs: a significant decrease in ROP, indicating the bit worn out and increase in electrodrill power consumption at the end of trip, with frequent spikes of WOB indicating bit bearing wear.

Due to low pressure in stand pipe during electrodrilling, it is recommended to create mud jet effect by using pump pressure in soft and medium formations while using roller cone, wing and diamond bits, that create significant pressure drop during drilling.

### **2.7.2 Application of Gaseous Mud Agents for Hole Cleaning**

As mentioned above, during electrodrilling, gaseous agents, including air, natural gas or exhaust gases, foams, suspensions and fogs can be used to remove the rock cuttings.

When using gaseous agents, well pressure is repeatedly reduced; bottom hole cleaning is improved; there is no filter cake on borehole, viscosity and solid particles content in blowing agent are sharply reduced; rock samples in form of uncontaminated mud are carried out by air to the surface in a very short time, water-producing oil-bearing and gas-bearing reservoirs are accurately drilled; there is no blockage of productive formation. The application of gaseous agents causes brief increase in ROP and bit durability: time spent on the preparation and drilling mud conditioning is eliminated, conditions for stripping of producing horizon are improved (Fomenko F.N., 1974).

However, in some cases, influx and cave-in control becomes more complicated, and risk of fires increases. These complications limit realization of the advantages listed above.

Therefore, method application should be followed by studying of geology. Drilling with aerated liquids is carried out when penetrating lost-circulation zones to improve bit performance, save material and technical means, as well as when stripping productive formations in order to preserve reservoir permeability and well stimulation time, as well as increase well productivity.

When cleaning of borehole with aerated mud, low values of WOB are required, therefore it is worth drilling at electrodrill terminal voltage of 10-15% lower compared to nominal one. This helps to limit the electrodrill heating.

Correction of voltage applied during drilling with blowing should be monitored by free running current. This value should be about 90% of free running current value set for drilling with well washing, it is recommended to determine the amount of air for drilled rock removal from the ensuring speed conditions for upward flow - at least 15 m/s (Fomenko F.N., 1974).

When drilling with blowing, special devices are used to seal wellheads, as well as backpressure valve in drill string.

## 2.8 Dynamic Loads

Dynamic loads caused by drill string vibration is one of the most undesirable problems encountered in drilling. It is important to control the level of vibration, otherwise they can lead to decrease in drilling efficiency or drilling tool damage. When designing a drill string for drilling using the electric drill, it is important to take into account the power conductors presence affection to dynamic loads. There are many ways to do this, among them: methods of active, passive and semi-active control of drill string vibrations (*Dong, G., Chen, P., 2016*).

There are three types of drill string vibration: axial, torsional and lateral. Torsional vibrations are accompanied by drill string twisting-unwinding, which leads to angular velocity increasing around the geometric central section. Axial vibration is represented by drill string movement along the vertical axis. Lateral vibrations are described by side movement of drill strings leading to its shocks. Lateral vibrations may lead also to damage of the drill string and borehole. (Dareing D.W., 1984).

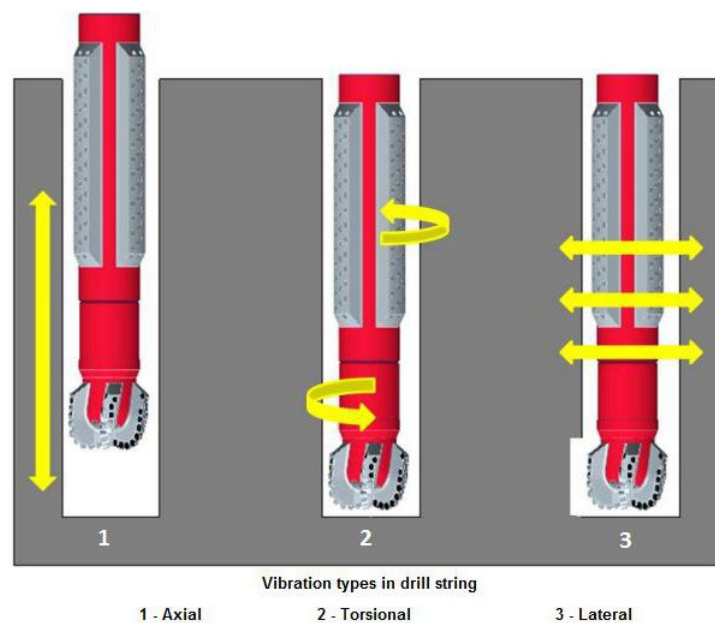


*Figure 2.7. Drill string vibration types.*

Each vibration form corresponds to certain geology, technology occurring condition. For instance, the drilling environment where longitudinal vibrations develop frequently is hard rock, application of PDM or roller cone bits. The typical condition when torsion vibrations develops: presence of salt, application of PDC bits with significant WOB. The typical conditions when lateral vibrations occur are soft formations, well with complex profile

(Dareing D.W., 1984). It should be noted that any form vibration occurrence depends on drilling modes chosen, bit – rock interaction, the presence of PDM and wellbore geometry.

Two ways of vibration estimation exist. One way is to establish the vibration model of drill string. This kind allows to predict some result, but, because of the complexity of drill string V&S, the predicted results may have a large deviation from actual results. The practical measuring method is the more effective evaluation method of drill string compare to the previous one. To receive dynamic data from the drill string, the modern measurement tools should be deployed (Dong, G., Chen, P., 2016).

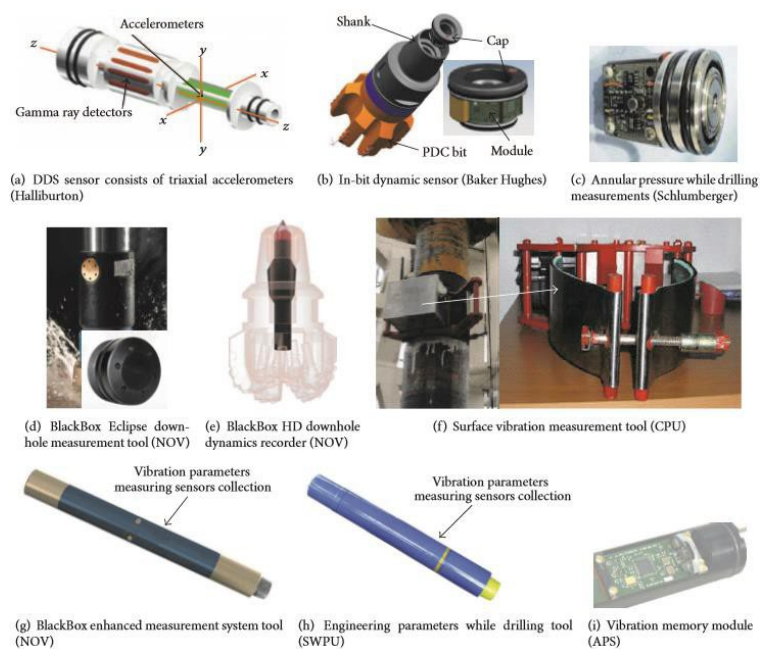


*Figure 2.8. Modern tool for drill string vibration detection  
(Dong, G. and Chen, P., 2016).*

Those are the modern vibration measurement tools in drilling engineering. These tools can provide with WOB, temperature, mud pressure, torque on bit, acceleration, revolutions per minute measuring (Dong, G. and Chen, P., 2016).

There are four main parts in the measurement system, bottomhole sensors (speed and acceleration sensor), data transferring, interpretation, and surface processing facilities.

In order to classify vibrations according to their severity and maximum possible duration, specialists from Halliburton, Baker Hughes, APS, NOV and Schlumberger have developed a special criterion based on field experience (Dykstra M.W. et al., 1984).

TABLE 3: Lateral vibration level classification.

Levels	Axial acceleration RMS (g)	Lateral acceleration RMS (g)	Limit time
Low	<1	<1	No
Medium	1~2	1~3	24 hours, suggest reducing vibration
High	2~4	3~6	12 hours, must reduce vibration
Severe	>4	>6	30 minutes, immediately reduce vibration

TABLE 4: Torsional vibration level classification.

Level	Stick-slip (/r/min)	State	Limit time
Low	0~40		No
Medium	40~60	Torsional vibration	No
Medium	60~80		Suggest reducing vibration
High	80~100	Stick-slip	Completely, must reduce vibration
Severe	>100	Stick-slip	30 minutes, immediately reduce vibration

Figure 2.9. Estimation criteria of drill string vibration (Dykstra M.W. et al., 1984).

There are three methods to control drill string vibration passive control, active control, and semiactive control.

### 2.8.1 Passive Control

Drill string passive vibration and shocks control of drill string means that control system does not require any additional energy other than that of the existing system. Resonance prevention is the most important method of passive drill string control. The main idea is the creation of math model, determination of natural frequency and, modal and harmonic analysis performing. The method aims to optimize the drilling parameters and reconsider BHA design to avoid the drill string resonance. Optimization of drilling dynamics is also effective approach to avoid drill string resonance (Dareing D.W., 1984). The relationship of WOB, RPM, and vibration for PDC bits was summarized in fig. 3.6 (Javanmardi K. Gaspard D. T, 1982).

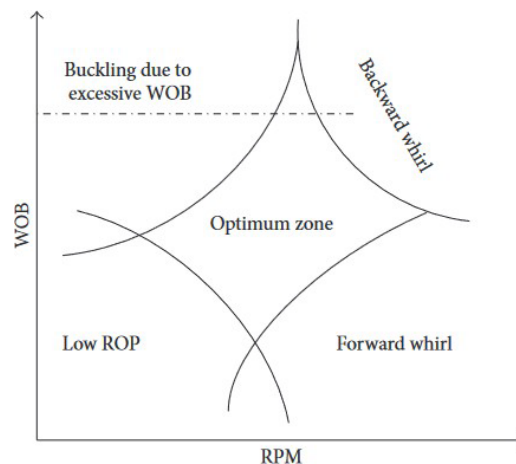


Figure 2.10. Optimum zone concept for PDC bits (Javanmardi K. Gaspard D. T, 1982.).

The area of the optimum zone depends on bit parameters and rock properties, but drill string dynamics significantly affects its size.

The other method of passive vibration control is the including of special equipment into drill string, e.g. antivibration bit with special structure design that can suppress or mitigate the vibration amplitude of drill bits. Decoupling of drill string stick-slip and whirl may be done by using of roller reamer. However, application of shock absorber is the most effective method of passive control, there are disc spring absorber and hydraulic absorbers included in drill string. (Dong, G. and Chen, P., 2016).



FIGURE 15: Hydraulic shock absorber.

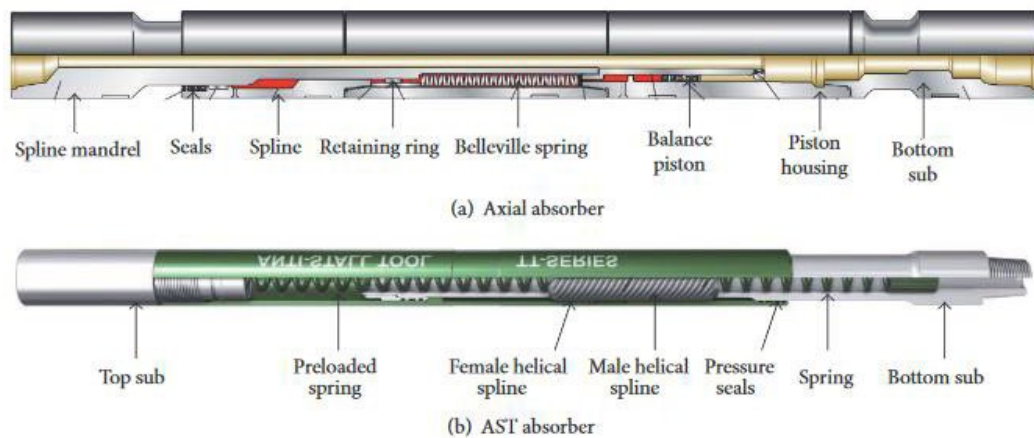


Figure 2.11. Typical V&S absorber (Dong, G. and Chen, P., 2016).

## 2.8.2 Active Vibration Control

In accordance with system dynamics control, vibration and shocks of the drill string is actively controlled by actively applying force equal and opposite to the forces generated by natural vibration. According to the relationship between the input and output of control system, the drill string system can be divided into open-loop and closed-loop feedback control systems. Open loop control aims to decrease or avoid external force completely. Closed-loop control aims to vary drill string stiffness and damping. Recently, vibration amplitude was reduced by automatically adjusting TOB and RPM is an important method (Dong, G. and Chen, P., 2016).

To monitor and control torsional vibration in drill string “soft” torque rotation system was introduced by Javanmardi and Gaspard. The detailed configuration and working principle of STRS is in Fig.3.8 (Javanmardi K., Gaspard D.T, 1982).

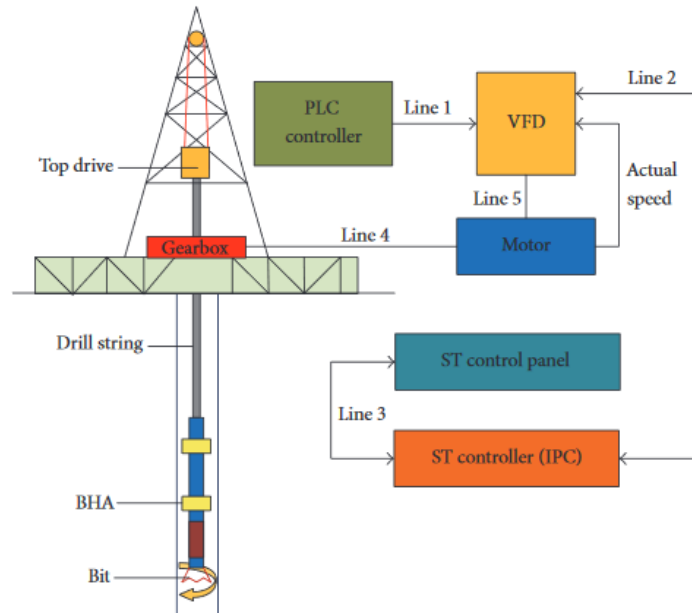


Figure 2.12. Soft torque rotation system configuration (Javanmardi K., Gaspard D. T, 1982).

This system is set in the top drive, and the vibration and shocks are managed by electric motors. The soft torque system applies compliance and damping to eliminate vibration instead of turning it into stick-slip. However, the system has some drawbacks: difficulties with calibration, substantial lag time. There will be other method considered for this reason.

### 2.8.3 Semiactive Vibration Control

Semiactive control technique has the pros over the mentioned control systems. To maintain an optimal state, semiactive control applying passive control tools requires less power to cure the system under consideration parameters and operating conditions. For instance, a semiactive vibration control damper was developed by APS. The tool chamber is filled with magnetic fluid the configuration of the tool is shown in fig.3.9. Vibration output is back to solenoid device, and vibrations and shocks are cured by changing the viscosity of magnetic fluid (Dong, G. and Chen, P., 2016).



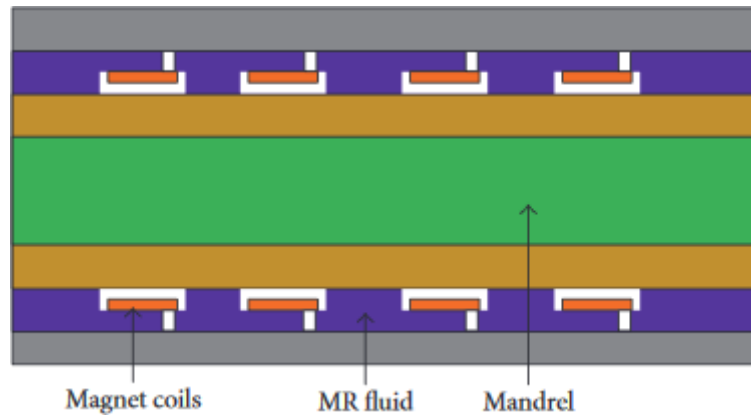


Figure 2.13. Semiactive vibration damper (Dong, G. and Chen, P., 2016).

#### 2.8.4 DYNTUB Software for Dynamic Loads Analyzing

The development of electrodrilling technology based on PMM requires dynamic loads estimation, which may occur in DPC due to the power conductors located inside. Based on the analysis results, it will be possible to create a test standard for this type of drill pipes on a special vibrostand simulating the real drilling conditions. After the tests, the possibility of DPC design optimization or need to apply the vibration prevention methods mentioned above will be considered. To analyze dynamic loads, it is proposed to apply DYNTUB program. Basic information about this software will be presented, including the equation of motion, boundary conditions and numerical method used in the software (Tikhonov V.S. et al, 2012).

DYNTUB considers the stiff dynamic model of drill string. The software allows taking into account the contact between wellbore and string, the pipes bending which occurred initially, interaction between PDC and the downhole under formation pressure, anisotropy of rock, sophisticated friction modelling of drill string, etc.

The main idea underlying the developed model of drill string is to take into account the elasticity of well wall. This accounting allows associating the contact force with the transverse displacement of drill string axis relative to the well axis. Therefore, the sophisticated and non-trivial task of contact force determination that affects the drill string in completely stiff walls of well was simplified to motion equations solving related to deformation. Quadratic-elastic model of pipe body wall lateral deformation was applied, in the considered formulas, which allowed numerical method to be more stable. The proposed approach significantly simplified the task of determining the contact zones and contact forces not only within the smooth sections of the drillstring, but also at the points of local thickenings: lock joints, stabilizers, centralizers (Tikhonov V.S. et al., 2014).

In buckling analysis, a longitudinal displacement or compressive axial displacement is given at the upper end of drill string, and an equation is given at the lower end that relates the bit load to the elastic deformation of the well bottom.

In order to examine drill string buckling phenomena during drilling, similar parameters of axial and lateral types are taken. WOB are defined at the bottom and angular velocity of drill string is given at the well surface.

When it comes to considering the directional well drilling with a bent sub by sliding mode, parameters of bending moment and longitude force to left and right of bend point are defined the string axis bend coordinate.

Equations of transverse forces applied on unit and appropriate parameters of transverse shaft and unit displacement at the beginning and end are defined. Additionally, coordinates of shaft displacement in system with no rotation unit are set for rotary steerable system application (Tikhonov V.S. et al., 2014).

It should be mentioned that boundary conditions involve cutting and friction force as well as torque applied on the bit dependences for all cases of wellbore trajectory calculations.

The axial and torsional motion equations are numerically integrated using the method of lines. Second order equations with respect to time, are converted to two equations of the first order, meaning partial derivatives with respect to length are approximated by finite, non-uniform differences in the mesh. Stability and accuracy are the main challenges that should be addressed when choosing an explicit numerical integration scheme. Timestep  $\Delta t$  is determined by the following equation.

$$\Delta t < \min \left( \Delta L^2 \sqrt{\frac{m^*}{EI}}, \sqrt{\frac{m^*}{\lambda}} \right);$$

*Figure 2.14.DYNTUB timestep (Tikhonov V.S. et al., 2012).*

where  $\Delta L$  - mesh size,  $\lambda$  - specific stiffness of the borehole wall, specified by Young's modulus  $E$ ,  $I$  - moment of inertia,  $m^*$  - effective mass of bottomhole assembly. Condition requires a very small timestep  $\Delta t$ , approximately  $10^{-4}$  to  $10^{-5}$  seconds, due to the material properties of drill string and BHA elements. This condition is not sufficient to numerically model processes that change quickly, such as drill string buckling problem. Integration timestep is capable of increasing by increasing  $m^*$  (Tikhonov V.S. et al., 2012).

The applying of this software to DPC dynamic loads analyzing will be considered in the next chapter.

## 2.9 Buckling in DP

The main limitation when drilling extended reach wells of small diameter wellbores are the resistance forces to movement and rotation of the drill string, overcoming which causes increased compressive forces and torque in drill string during the transfer of axial load and torque to bit.

The most dangerous consequence of the compressive loads action is the local loss drill sting longitudinal stability, first in the form of sinusoid. Then, as compressive load increases, drill sting deforms into spatial spiral. Excess of compressive forces in excess is accompanied by progressive increase in the contact forces which leads to stuck of drill sting. Drill string buckled form can vary depending upon many factors (Mitchel R.F, 2002).

Most often, "buckling" is observed when drilling in "sliding" mode, i.e. without rotating the drill sting. When drilling with rotary systems, "buckling" also manifests itself in the forms of an oscillating flat sinusoidal or spatial form, planetarily rolling around well axis.

Traditional formula applied to predict helical buckling is showed below (Menand S. et.al., 2019).

$$F_{hel} = k \sqrt{\frac{EI\omega \sin(Inc)}{r}}$$

*Figure 2.15. Critical force for helical buckling. (Menand S. et.al., 2019).*

The k number varies from 2.83 to 5.65, depending on the author and on the different assumptions made. The k number is responsible for shape of drill string in the borehole. It should be mentioned that this simplified formula is only applicable in idealized cases. In fact, to account for buckling in wellbore the many factors should considered: wellbore tortuosity, trajectory, dogleg severity. Simple equation is not capable of describing such sophisticated problem (Menand S. et.al, 2019).

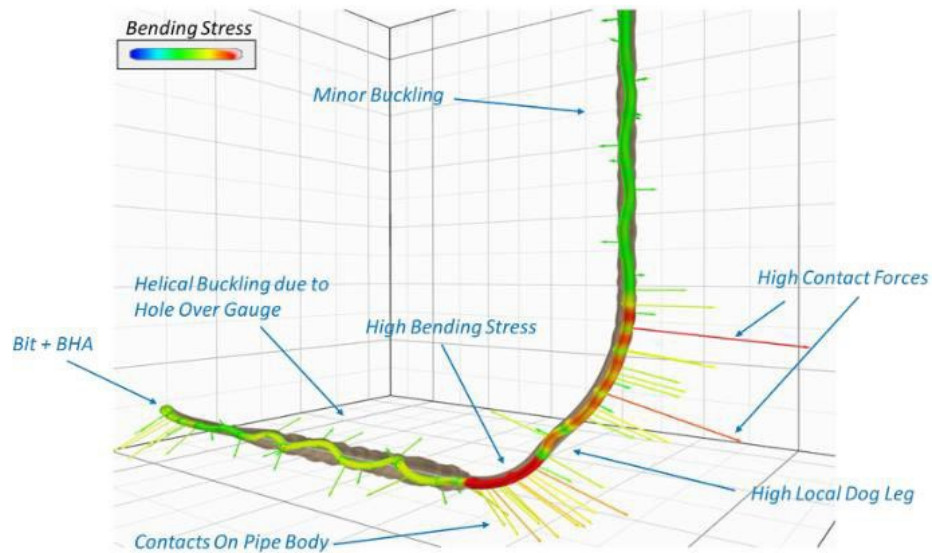


Figure 2.16. Buckling behavior (Menand S. et.al, 2019).

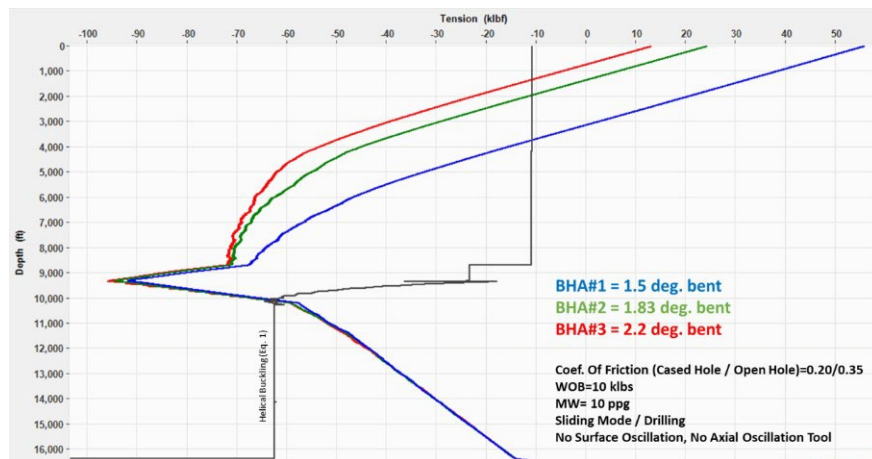


Figure 2.17. Tension/Compression along the drill string while drilling (Menand S. et.al, 2019).

In Fig.3.13 a comparison between 3 different BHAs is represented meaning there are different sliding behavior with the similar weight on bit. It's interesting to notice that there is about 40klbs tension difference at surface between the trajectories drilled by BHA#1 and by BHA#3. In other words, tension in drill string may significantly vary depending upon dogleg severity.

Buckling is quite sophisticated problem meaning that a small change in parameter which are corresponding to drilling can affect results significantly. One recommends generally running all simulations with several coefficients of friction as high as 0.4 or even 0.5 to anticipate any potential problems such as lock-up (Menand M., Farrag M., 2019).

### 2.9.1 Buckling in DPC

Buckling may lead to drilling process complications or its stop. Therefore, it is necessary to apply special equipment and methods capable of preventing those events. DYNTUB and Landmark software allow to evaluate drill pipes buckling resistance in relation to a specific well with given parameters. The software can also be used for DPC since their design do not have significant differences from standard drill pipes that would affect buckling. After analyzing this phenomenon, traditional methods of its prevention can be applied: increasing of wall thickness, outer diameter in drill string areas subjected to buckling, application of DP manufactured of other steel groups, application of aluminum DP to reduce the friction in inclined and horizontal intervals of the wellbore, changing the wellbore trajectory.

### 2.10 Features of DPC Hydraulic Analysis

As presented earlier in this chapter, the modern electric drill pipes developed by Novobur LLC have differences compared to standard drill pipes and previous generation electric ones that will affect the hydraulic characteristics of such pipes. DPC-102 has smaller diameter compared to traditional drill pipes of the same unit size, due to presence of cylindrical sleeve in pipe body wall, however, this feature does not complicate the hydraulic analysis. The feature of DPC-127 is power conductors on pipe inner wall, whose presence increases the hydraulic losses inside drill string. In order to assess the hydraulic losses when using DPC-127, it is necessary to provide calculation of equivalent (hydraulic) diameter of a noncircular cross section. The essence of this technique is to calculate the diameter of a smooth pipe, whose diameter depends on the noncircular flow section size of DPC-127 (Altshul A., 1982). It should be noted that the power conductors inside in this case acts not as an obstacle that creates local resistance to mud flow, but as an object which changes the shape of flow cross section. Below is equivalent diameter calculation for DPC-127.

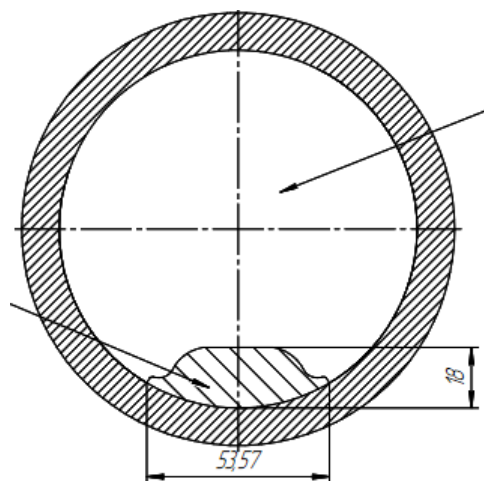


Figure 2.18. Cross-section of DPC-127 (inner diameter-105mm) (Novobur LLC).

The area of the effective cross-section will be calculated as follows:

Area of obstacle:

$$S_{obstacle} \approx \frac{18 \cdot 53,57}{10^6} \cdot 0,8 \approx 0,77 \cdot 10^{-3} m^2 \quad (2.1)$$

Area of effective cross section:

$$S_{effective\ cross-section} \approx \frac{\pi \cdot 0,105^2}{4} - S_{obstacle} \approx 0,789 \cdot 10^{-2} m^2 \quad (2.2)$$

Wetted perimeter:

$$P = 105 \cdot \pi + 2 \cdot 18 = 0,2937m \quad (2.3)$$

Hydraulic radius:

$$R_h = \frac{S_{effective\ cross-section}}{P} = 21,38mm \quad (2.4)$$

Hydraulic diameter:

$$D_h = 4 \cdot R_h = 85,52mm \quad (2.5)$$

The calculated equivalent diameter will be used in hydraulic analysis in the next chapters of master's thesis.

## 2.11 Summary

In this chapter, the new DPC design developed by Novobur LLC was considered. The main feature of DPC-127 is the presence of power conductors on the pipe body inner wall, which can affect the dynamic loads in drill string and hydraulic program characteristics.

The features of drilling technology using an electric motor were presented and overview of dynamic loads that occur in drill string, as well as methods for their assessment and prevention, were presented. For the analysis of dynamic loads, application of DYNTUB program is proposed, standard for testing DPC on the vibrostand of Novobur LLC will be developed based on the results, details will be presented in the next chapter. Also, the method

for hydraulic losses estimation in DPC-127 was presented. Based on this method, comparative hydraulic analysis of DPC and standard drill pipes application will be carried out in the next chapter.

## Chapter 3

### DPC Analytical Studies

This chapter will present the initial data and the analytical studies results of hydraulic losses and dynamic loads occurring due to the current design features of DPC.

#### 3.1 Comparative Hydraulic Analysis of DPC and Traditional Drill Pipes

In this section, comparative hydraulic analysis of pressure losses is performed when drilling for intermediate casing with an outer diameter of 178 mm using PDM and RSS (the drill string consists of conventional DP-127x9,19) and during electric drilling (the drill string consists of DPC – 127 or DPC-140). Also, hydraulic analysis is carried out in DP-102x8 and DP– 102 drill strings when drilling for liner with a diameter of 114 mm. WellPlan (Landmark) software will be used for the analysis, as well as standard formulas for calculating the hydraulic losses (the results of these calculations will be placed in brackets).

##### 3.1.1 Hydraulic Program Analysis of 178 mm Intermediate Casing Drilling with DP-127.

Before the start, the assumptions applied for DPC-102, DPC-127, DPC-140 should be considered.

In the analysis, the previously calculated hydraulic diameter of DPC-127 was used. When calculating pressure losses in annulus for DPC-127 and DPC-102, outer diameter of the drill pipes and tool joints was used, which were taken from the drawings provided by Novobur LLC.



Since in this calculation it is proposed to use DPC-140, manufacture of which will be proposed later, inner and outer diameters of those were preliminary taken proportionally with those of DPC-127.

Pressure drop for PDM and RSS will be presented in tables, the pressure drop of PMM in all cases was assumed to be 0.5 MPa.

The analysis will be performed for the given water based mud (WBM) with Bingham plastic rheological model, which will be marked with an «\*» in the analysis results. Application of oil-based mud (OBM) and Herschel-Bulkley rheological model will also be considered.

When considering the application of RSS and PDM in BHA, mud flow rate was chosen based on effective hole cleaning conditions. Minimal acceptable flow rate was set for PDM exploitation (Leonov E., Simonyants S., 2014).

It should be noted that results based on the standard methodic showed pressure losses increasing compared to WellPlan analysis. This is explained by power dependences between tool joints diameter and pressure losses, that is, insignificant decreasing of diameter leads to significant pressure losses increasing.

*Table 3.1. Initial data for hydraulic analysis of intermediate casing with a diameter of 178 mm.*

Parameter	Value	Unit
TVD	2062	m
MD	2727	m
Bit diameter	0,2207	m
Cavernosity coefficient	1,1	-
Well diameter	0,231	m
DP for drilling with RSS and PDM		
Outer diameter of DP-127	0,127	m
Inner diameter of DP-127	0,109	m
Length of DP-127 section	2550	m
Outer diameter of tool joints ZU-155	0,155	m
Inner diameter of tool joints ZU-155	0,095	m
Pressure losses in PDM-172	8,7	MPa
Pressure losses in RSS (RSM675)	1	MPa
Drilling with PMM (DPC-127)		
Hydraulic diameter (inner) for WDP-127	0,08552	m
Outer diameter of DPC-127	0,127	m
Outer diameter of tool joints	0,168	m
Inner diameter of tool joints	0,061	m

Length of DPC-127 section	2550	m
Pressure losses in PMM-172	0,5	MPa
Drilling with PMM (DPC-140)		
Hydraulic diameter (inner) for DPC-140	0,0995	m
Outer diameter of DPC-140	0,140	m
Outer diameter of tool joints	0,178	m
Inner diameter of tool joints	0,071	m
Length of DPC-140 section	2550	m
Pressure losses in PMM-172	0,5	MPa

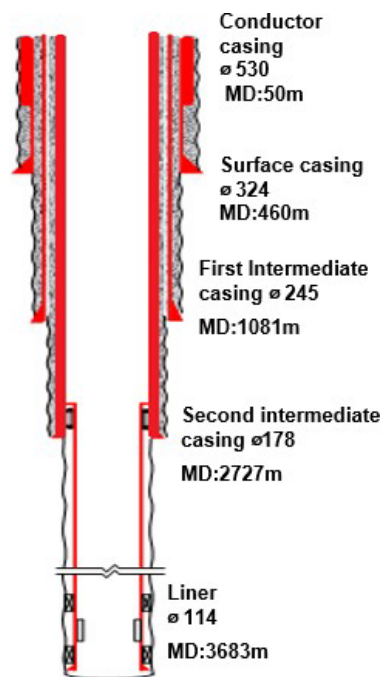


Figure 3.1. Well design (Novobur LLC).

Table 3.2. Pressure losses while drilling for 178 mm intermediate casing (\* - Given mud; results in brackets are obtained by standard methodic ).

Mud type	Density [ $\frac{kg}{m^3}$ ]	Rheology model	Yield point [Pa]	n'	K'	Plast.visc. [mPas]	PDM		PMM (DPC-127)		PMM (DPC-140)		RSS	
							Drill string losses [MPa]	Total losses [MPa]	Drill string losses [MPa]	Total losses [MPa]	Drill string losses [MPa]	Total losses [MPa]	Drill string losses [MPa]	Total losses [MPa]
WBM*	1150	Bingham plastic	7	-	-	23,9	16,835	22,121	18,124	22,954	11,788	16,868	9,135	14,421
WBM	1150	Hershel-Bulkley	7	0,6	0,49	-	(16,44)	(21,21)	(20,7)	(25,82)	(11,47)	(16,39)	(9,44)	(13,5)
OBM	900	Bingham plastic	2	-	-	12,2	14,194	17,750	12,912	16,135	9,549	11,851	6,494	10,050
OBM	900	Hershel-Bulkley	2	0,6	0,49	-	14,755	18,904	12,881	16,921	8,779	13,147	7,055	11,204

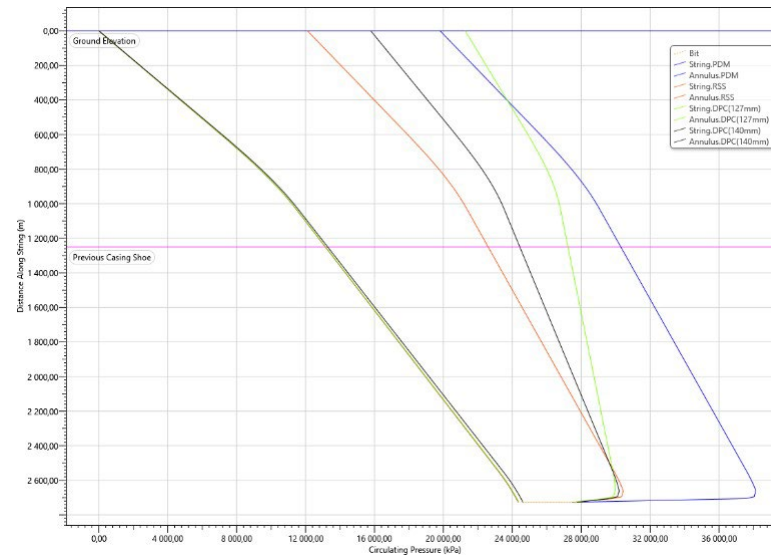


Figure 3.2. Pressure distribution along the wellbore.

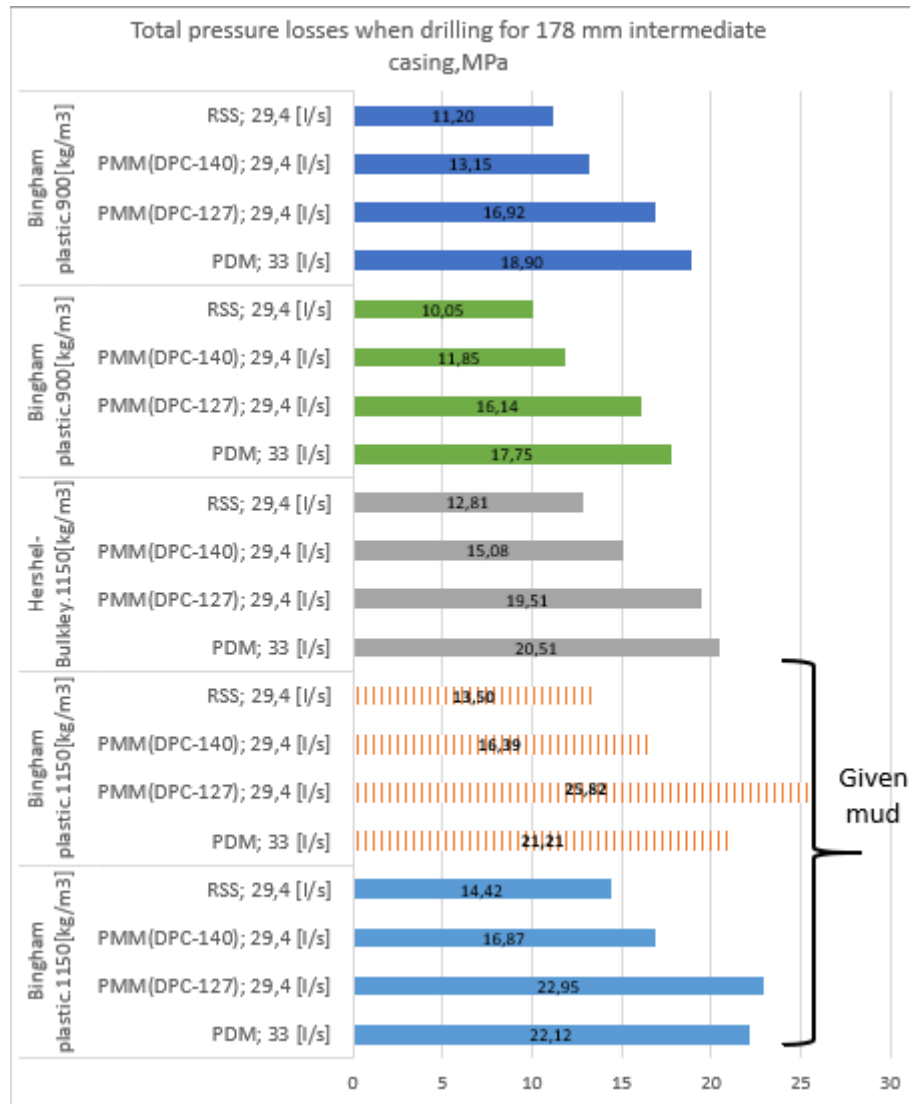


Figure 3.3. Interrelation of total pressure losses (standard methodic results are shaded).

Based on WellPlan results for the given mud, it can be seen that the pressure loss when using PMM (DPC-127) is approximately 4% higher compared to PDM. The difference between RSS and PMM (DPC-127) is approximately 45,6%.

Application of standard methodic, results of which are presented with shading, showed the greater difference in pressure losses due to the presented reasons – 11,75% between PMM (DPC-127) and PDM, and 62% between PMM (DPC-127) and RSS.

It is known that DP with outer diameter of 140-147 mm have a superior hydraulic performance compared to DP-127. For this reason, application of DPC-140 was considered, pressure losses in which turned out to be 24% less compared to PDM and 15% higher in comparison with RSS in accordance with WellPlan results. It will be recommended to create DPC with an outer diameter of 140 mm in the future.

It should be noted that the application of different rheological models and OBM for predicting pressure losses shows hydraulic performance improvement for all types of DP under consideration.

### 3.1.2 Hydraulic Program Analysis of 114 mm liner Drilling with DP-102.

*Table 3.3. Initial data for 114 mm liner drilling.*

Parameters	Value	Unit
TVD	2069	m
MD	3683	m
Bit diameter	0,156	m
Cavernosity coefficient	1,1	
Well diameter	0,163	m
DP for drilling with PDM and RSS		
Outer diameter of DP-102 (with inner upset)	0,102	m
Inner diameter of DP-102	0,086	m
Length of DP-102 section	3555	m
Outer diameter of tool joints ZSH-133	0,133	m
Inner diameter of tool joints ZSH-133	0,072	m
Pressure losses in PDM-120	9	MPa
Pressure loss in RSS SureSteer™475	1,5	MPa
DP for drilling with DPC		
Outer diameter of DPC-102	0,102	m
Hydraulic diameter (inner) for DPC-102	0,069	m
Length of WDP-102 section	3555	m
Outer diameter of tool joints	0,133	m
Inner diameter of tool joints	0,048	m
Pressure losses in PDM-120	0,5	MPa
Depth of previous casing shoe	2727	m
Inner diameter of the casing	0,169	m

Table 3.4. Pressure losses while drilling for 114 mm liner (\* - Given mud; results in brackets are obtained by standard methodic).

Mud type	Density [ $\frac{kg}{m^3}$ ]	Rheology model	Yield point [Pa]	n'	K'	Plast.visc. [mPas]	PDM		PMM (DPC-102)		RSS	
							Drill string losses [MPa]	Total losses [MPa]	Drill string losses [MPa]	Total losses [MPa]	Drill string losses [MPa]	Total losses [MPa]
WBM*	1150	Bingham plastic	7	-	-	23,9	20,312 (21,54)	27,574 (28,77)	18,681 (22,6)	26,312 (29,32)	12,812 (14,04)	20,074 (21,27)
WBM	1150	Hershel-Bulkley	7	0,6	0,49	-	18,739	26,112	15,645	23 101	11,239	18,612
OBM	900	Bingham plastic	2	-	-	12,2	16,542	21,885	12,808	17,952	9,042	14,385
OBM	900	Hershel-Bulkley	2	0,6	0,49	-	17,326	23,981	13,410	20,196	9,826	16,481

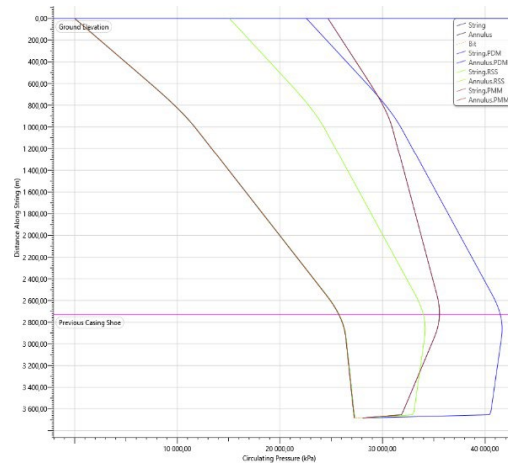


Figure 3.4. Pressure distribution along the wellbore.

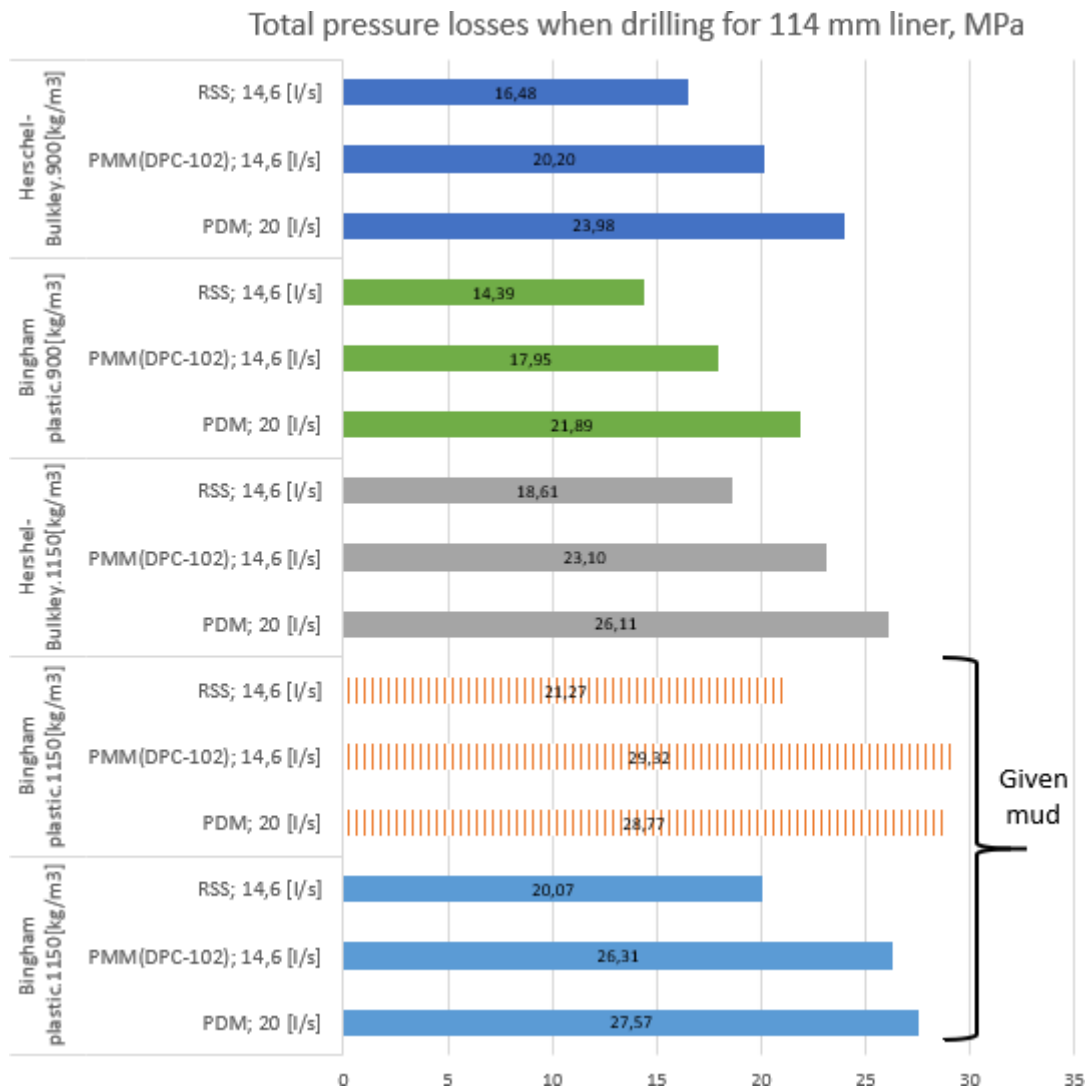


Figure 3.5. Interrelation of total pressure losses (standard methodic results are shaded).

### 3.1.3 Results of Hydraulic Analysis

It was shown that pressure losses increase significantly when compared with RSS in the case of PMM (DPC-127) application for intermediate casing drilling. However, the difference in pressure losses is insignificant compared to PDM due to pressure drop on it. Additional pressure losses in DPC-127 are explained by decrease in the pipe body and tool joints flow area.

Application of DPC-102 for 114 mm liner electric drilling reduces the total pressure losses by 5% and increases by 24% when compared with PDM and RSS, respectively. This increase in pressure loss is also due to the above reasons.

The presented calculations indicate pretty significant increases in pressure losses for DPC-127, which may affect comparative efficiency of the proposed drilling method. To

improve the hydraulic characteristics, variant of DPC-140 with larger diameter manufacturing is proposed, which is also applicable when drilling wells with diameter of 220 mm.

It should be noted that equivalent diameter concept does not describe DPC geometry accurately. To clarify the affection of power conductors on pressure losses, experimental tests will be carried out at NMPSE, as well as flow simulation in DPC via OpenFOAM software. According to test results, it will be possible to conclude that DPC application allows to improve the hydraulic characteristics during drilling.

## **3.2 DPC Pressure Losses Analysis via OpenFOAM**

### **3.2.1 OpenFOAM Application Justification and Analysis Methodic**

The decision to apply this software was made due to insufficient accuracy of power conductors accounting methodology in DPC-127. The analytical solution method is very accurate in case of considering simple problems of fluid flow in smooth pipes. However, when changing the drill pipes body geometry, it is necessary to compare the results of calculating pressure losses in DPC-127 obtained analytically with numerical (OpenFOAM) and experimental (details in the next chapter) results. By comparing the results obtained, it will be possible to judge about applicability of the equivalent diameter concept.

It should be noted that numerical method advantages of pressure drop calculating in OpenFOAM over the analytical one is possibility of considering the flow area with complex geometry, various rheological flow models and boundary conditions.

However, there are disadvantages: as problem complexity under consideration increases, it is necessary to increase the computing resources; the calculation time can reach from several hours to a day.

To analyze pressure losses, it is proposed to apply OpenFOAM software (Open Source Field Operation and Manipulation CFD ToolBox) — an open integrated platform for numerical modeling of continuum mechanics problems. OpenFOAM provides with solving of Navier-Stokes equation for virtually any kind of fluid. Also turbulence can simulated there using various models (CFD Direct, 2022).

To calculate the pressure drop in DPC-127, the solution of Navier-Stokes equations for an incompressible fluid will be considered (the density of the fluid is unchanged). Equations and calculation methods are presented below.



$$\underbrace{\frac{d\bar{u}}{dt}}_{\text{Inertia forces}} = \underbrace{\bar{F}}_{\text{External forces}} - \underbrace{\text{grad } p}_{\text{Pressure forces}} + \underbrace{\mu \nabla^2 \bar{u}}_{\text{Viscous forces}}$$

$$\text{div } \bar{u} = 0$$

Figure 3.6. Navier-Stokes equations for an incompressible fluid (Hpc-educaiton, 2011)

To solve Navier-Stokes equation in relation to mud flow in DPC-127, OpenFOAM will implement SIMPLE (Semi-Implicit Method for Pressure-Linked Equations) algorithm, which allows linking the Navier-Stokes equations with an iterative procedure. The iterative procedure is presented as follows (Hpc-educaiton, 2011).

1. Setting boundary conditions.
2. Solving of discretized momentum equation to obtain an intermediate velocity field.
3. Calculating of mass flow through the cell faces.
4. Solving of pressure equation with using relaxation coefficients.
5. Clarifying of mass flow through the cell faces.
6. Speed clarifying based on new pressure field.
7. Updating the boundary conditions.
8. Repeating until convergence.

Steps 4 and 5 can be repeated several times to correct non-orthogonality of calculated mesh.

It is known that in almost all cases, drilling mud flow in drill pipes is turbulent. To account for turbulence in OpenFOAM, k-omega SST turbulence model will be applied. Benefit of this model is that it allows simulating a flow with  $y^+$  values in a wide range. " $Y^+$ " is a dimensionless value that characterizes distance from the wall to the nearest mesh node. This parameter depends on calculated mesh density near wall. Knowing this parameter, it is possible to determine in which region (viscous, logarithmic or buffer layer) the flow simulation takes place (CFD Direct, 2022).

### 3.2.2 Task Description and Initial Data

Aim of this work is to estimate affection of power conductors presence on pressure losses in DPC.

To achieve the aim, two pipe designs will be considered: conventional DPC (with power conductors inside) and the same drill pipes, but without power conductors (DPCW). Pipe body duct of the drill pipes will be simulated with mud passing through it. OpenFOAM

software will be applied to perform the simulation and measure the pressure losses. Before OpenFOAM simulation the analytical hydraulic loss calculation will be performed to compare results at the end.

*Table 3.5. Initial data for analytical calculations and simulation.*

Parameter	Value		Unit
	DPC	DPCW	
Diameter of pipe body duct, d	0,08552 (analytical)	0,105	m
	0,105(OpenFOAM)		
Length of duct, L	10,5		m
Mud properties			
Rheology model	Bingham plastic		-
Density, $\rho$	1150		kg/m <sup>3</sup>
Yield strength, $\tau_0$	7		Pa
Plastic viscosity, $\eta$	23,9		mPa
Flow rate, Q	30		liters/s

As presented above, different diameters of pipe body duct will be used. Analytical calculations require the equivalent diameter of DPC to estimate pressure losses. OpenFOAM simulation requires initial boundary and field conditions estimated with the help of DPCW diameter. After simulation, there will be an opportunity to clarify the equivalent diameter of DPC-127.

### 3.2.3 Analytical Calculations

It should be noted that DPC has the equivalent diameter in this calculation, which accounts for the cable inside. Standard formulas for hydraulic losses as well as WellPlan (Landmark) software were used in these calculations.

Table 3.6. The results of analytical calculations.

Parameter	Value		Unit
	DPC	DPCW	-
$Re_{cr}$	8001	9587	-
Re	35837	29188	-
Hydraulic resistance coefficient, $\lambda_r$	0,0298	0,0295	-
$\Delta P$ stand.	159,69	56,66	kPa
$\Delta P$ WellPlan	123,05	46,43	kPa

It can be seen that pressure losses in DPC are approximately 2,7 times higher compared to DPCW at the same flow rate for two types of calculations. However, the concept of equivalent diameter is not accurate enough. OpenFOAM simulation should provide with more precise results for the given geometries and flow rate.

### 3.2.4 Estimation of Hydraulic Losses via OpenFOAM Software

To create geometry for DPC and DPCW, Salome software was used. Also, groups of faces were chosen to create the boundary conditions in OpenFOAM. Axis of pipes was aligned with OX. There will be symmetry exploited, therefore the half of both pipes is needed only.

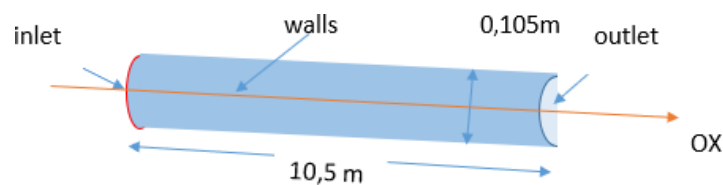


Figure 3.7. Model of DPCW and names of its faces.

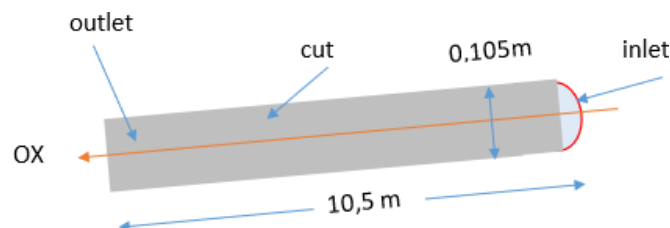


Figure 3.8. The other side of DPCW (where "cut" face is located).

The geometry for DPC is almost the same but there is a cutout at the pipe periphery representing the power conductors location (fig.3.2.3).

After geometry creation, the pipes should be meshed. The mesh parameters are as follows.

*Table 3.7. Mesh parameter for DPC and DPCW.*

	DPC	DPCW
Algorithm	3D Automatic Tetrahedralization	
Length (mean size)	0,006	
Number of 1D (edges)	4086	2089
Number of 2D (faces)	96 896	105 082
Number of 3D (volumes)	496 956	498 658

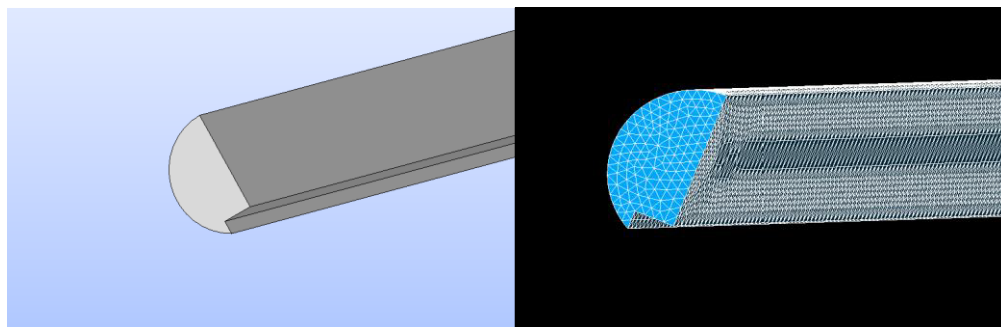


*Figure 3.9. left) DPC geometry and right) DPC after meshing.*

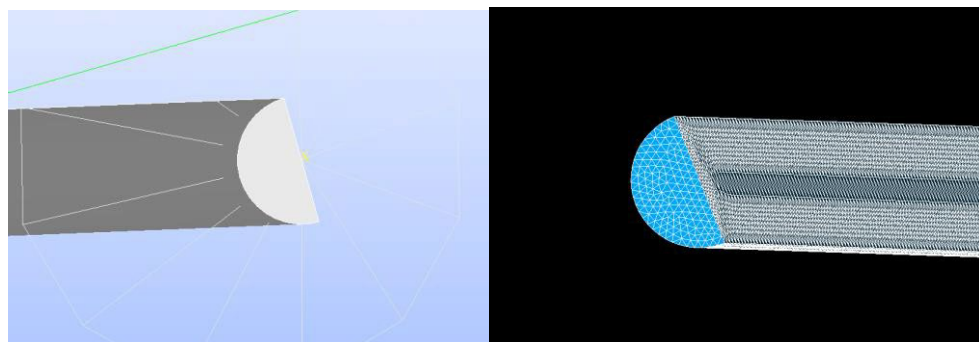


*Figure 3.10. left) DPCW geometry and right) DPCW after meshing.*

After meshing, command of “polyDualMesh -concaveMultiCells 60” was implemented to transform tetrahedral mesh to polyhedral one for both pipe designs. «CheckMesh» utility showed the following mesh problems:

*Table 3.8. Mesh problems.*

DPC	DPCW
1) Number of severely non-orthogonal (> 70 degrees) faces: 154.	Number of
2) Number of non-orthogonality errors: 12.	severely non-
3) Error in face pyramids: 29 faces are incorrectly oriented.	orthogonal (> 70 degrees)
4) Max skewness = 263.78, 22 highly skew faces detected	faces: 12.

To cure DPC mesh problems 2 additional non-orthogonality corrections were implemented within a single global iteration to analyze the pressure field.

### 3.2.5 Initial Data for OpenFOAM Simulation

Before the simulation, initial boundary and internal field condition have to be set. Turbulent kinetic energy and other parameters were determined with the help of following equations (*CFD Direct, 2022*). Velocity (3,46 m/s) was calculated for the given flow rate (30 liters/s), which corresponds to the flow rate considered in experimental part of master thesis.

Initial turbulence intensity is given by:

$$\begin{aligned}
 I &= 0,16Re^{-\frac{1}{8}} = \\
 &= 0,16 \cdot \left(\frac{\rho \cdot U \cdot d}{\eta}\right)^{-\frac{1}{8}} = 0,16 \cdot \left(\frac{1150 \cdot 3,46 \cdot 0,105}{0,0239}\right)^{-\frac{1}{8}} = 0,044
 \end{aligned} \tag{3.1}$$

where Re - Reynolds number,  $\rho$  – density of mud,  $U$  – mean velocity,  $\eta$  – plastic viscosity,  $d$  – diameter of duct.

Turbulent kinetic energy is given by:

$$k = \frac{3}{2}(UI)^2 = 1,5 \cdot (3,46 \cdot 0,044)^2 = 0,097 \left(\frac{m^2}{s^2}\right) \tag{3.2}$$

Turbulent length scale is represented by:

$$l = 0,07 \cdot L = 0,07 \cdot 0,105 = 0,00735 \text{ (m)} \tag{3.3}$$

where L – diameter of pipe duct.

Specific dissipation is given by:

$$\omega = \frac{k^{0,5}}{c_{\mu}^{0,25}l} = \frac{0,097^{0,5}}{0,09^{0,25}0,00735} = 77,7 \left(\frac{1}{s}\right) \tag{3.4}$$

where  $c_{\mu}$  is a  $k$ -parameter which is equal to 0,09.

Boundary and internal field conditions for initial time are presented below.

Table 3.9. Boundary and internal field conditions

	U	P	omega	k	nut
Inner field	uniform (0 0 0)	uniform 0	uniform 77,7	uniform 0.0444	uniform 0
Inlet	flowRateInletVelocity; volumetricFlowRate 0.03;	zeroGradient	turbulentMixingLengthFrequencyInlet; mixingLength 0.00735; inletOutlet;	fixedValue; uniform 0.0444	calculated uniform 0;
Outlet	zeroGradient	fixedValue uniform 0	inletValue \$internalField;	zeroGradient	calculated uniform 0;
Walls	noSlip	zeroGradient	omegaWallFunction;value \$internalField;	kqRWallFunction; uniform 0.0444	nutkWallFunction; uniform 0
Cut			symmetryPlane		

As was presented in initial data mud flow will be described with Bingham plastic model. To set this model in simulation, Herschel-Bulkley transport model should be used, which has the following form in OpenFOAM.

$$\mu = \min \left( \mu_0, \frac{\tau_0}{\dot{\gamma}} + k\dot{\gamma}^{n-1} \right) \tag{3.5}$$

Where  $\dot{\gamma}$  – shear rate,  $k$  – consistency index,  $\mu$  – viscosity,  $\mu_0$  – initial viscosity,  $n$  – flow index,  $\tau_0$  - threshold stress.

To convert Herschel-Bulkley into Bingham plastic model flow index «n» has to be equal to value of «1» (CFD Direct, 2022).

Transport model, turbulence and case control properties for the simulation are presented below. It should be noted that flow model parameters in OpenFOAM are expressed in basic (fundamental) units of measurement expressed mud density in this case.

*Table 3.10. Transport model, turbulence and case control properties.*

Parameter	Value	Unit
Case control properties		
Start time	0	-
End time	100	-
deltaT	1	-
Transport model	Herschel-Bulkley	
$\mu_0$	$1 \cdot 10^{-3}$	$\text{m}^2/\text{s}$
$\tau_0$	$6.08 \cdot 10^{-3}$	$\text{m}^2/\text{s}^2$
k	$2.07 \cdot 10^{-5}$	$\text{m}^2/\text{s}$
n	1	-
Turbulence model	RAS; k-omega SST	-

Mud will be assumed as incompressible. The stable state simulation will be considered with simpleFoam solver aimed for steady state flow simulation.

### 3.2.6 Results of Simulation

After performing the simulation, following results were obtained. Pressure difference was calculated by special command «pressureDifferencePatch» which subtracts the inlet pressure from outlet one. Results are presented for the moment when residuals reached the set value ( $10^{-5}$ , [m<sup>2</sup>/s<sup>2</sup>]).

*Table 3.11. Results of simulation.*

Parameter	Value		Unit
	DPC	DPCW	
Kinematic pressure losses	50,1	39,2	$\text{m}^2/\text{s}^2$
Pressure losses	57,6	45,1	kPa

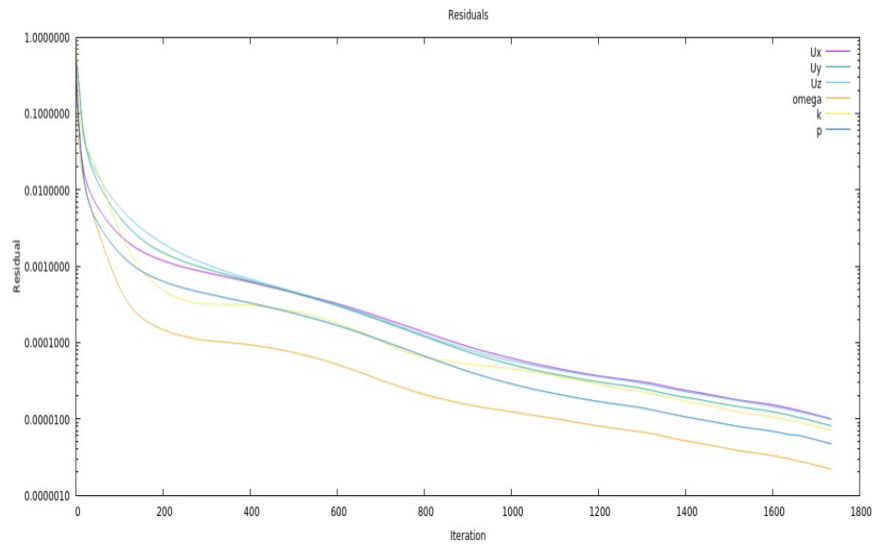


Figure 3.11. Residuals for DPCW case.

### 3.2.7 Result Comparison

The results of simulation are in table 4.10. and fig.4.14.

Table 3.12. Result comparison.

Parameter	Value		
	DPC	DPCW	Additional pressure losses due to power conductors, kPa
Standard formulas $\Delta P, kPa$	60,6	21,8	38,8
WellPlan analysis, kPa	50,4	18,9	31,4
OpenFOAM simulation $\Delta P, kPa$	57,6	45,1	12,5



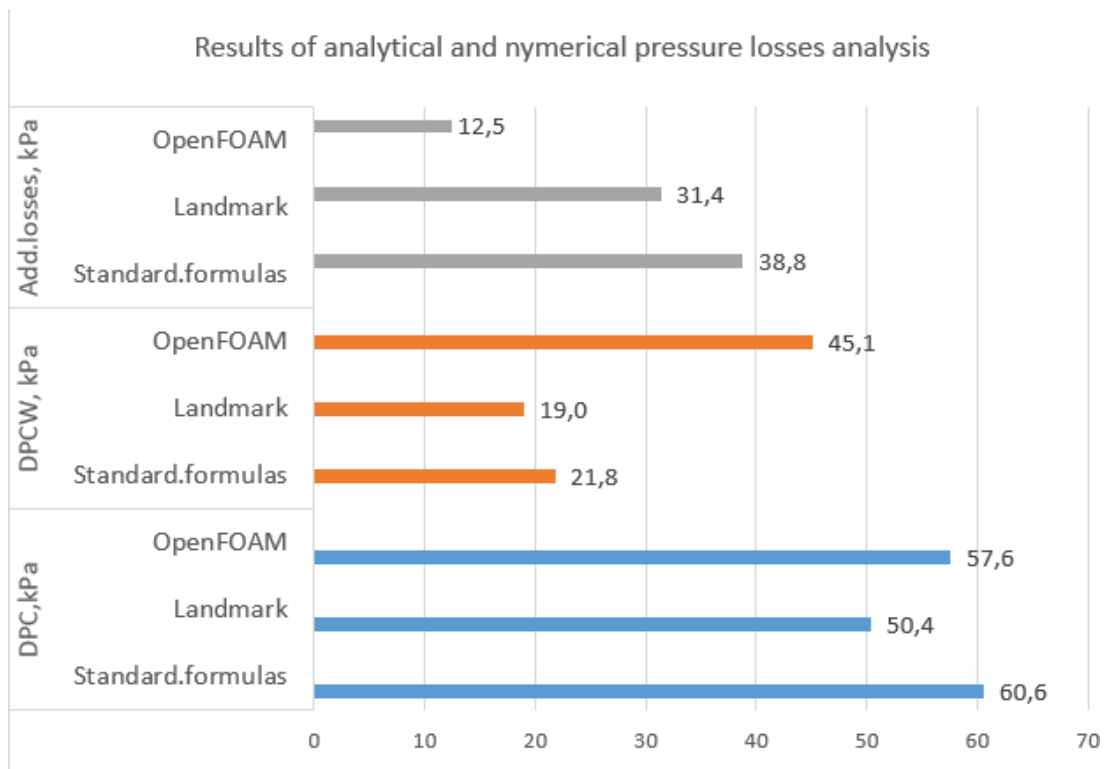


Figure 3.12. Results of analytical and numerical pressure losses analysis.

OpenFOAM shows that affection of cable accounts for 12,5 kPa which is not high compared to the standard formulas and WellPlan analyzing. Other calculation methods show an increase in the losses by more than 2,5 times compared to DPCW, which is quite significant value considering the power conductors size.

It is worth paying attention to the case of DPCW, in which there are no power conductors in flow area. It may be said that standard formulas and calculations in WellPlan should show the most accurate results in this case. The calculation in OpenFOAM shows an increase in pressure by about 2 times compared to the analytical calculation, however, this does not indicate the inapplicability of the model created in OpenFOAM. Perhaps the numerical method shows greater pressure loss results than it actually is, but it should be noted that this software describes the phenomenon of turbulence and non-Newtonian fluids flow compared to the previous ones more accurately.

One reason of slight overestimation in DPCW case is non-steady state flow at DPCW inlet because of constant flow rate boundary condition. The overestimation does not exceed the 1 kPa. The velocity distribution (fig.3.13) at outlet, side view of velocity profile and pressure distribution along the pipe (fig.3.14) are depicted in following figures.

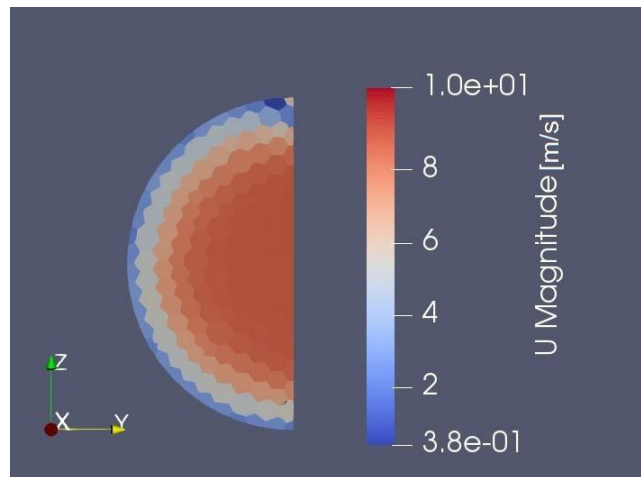


Figure 3.13. Velocity distribution at outlet of DPCW.

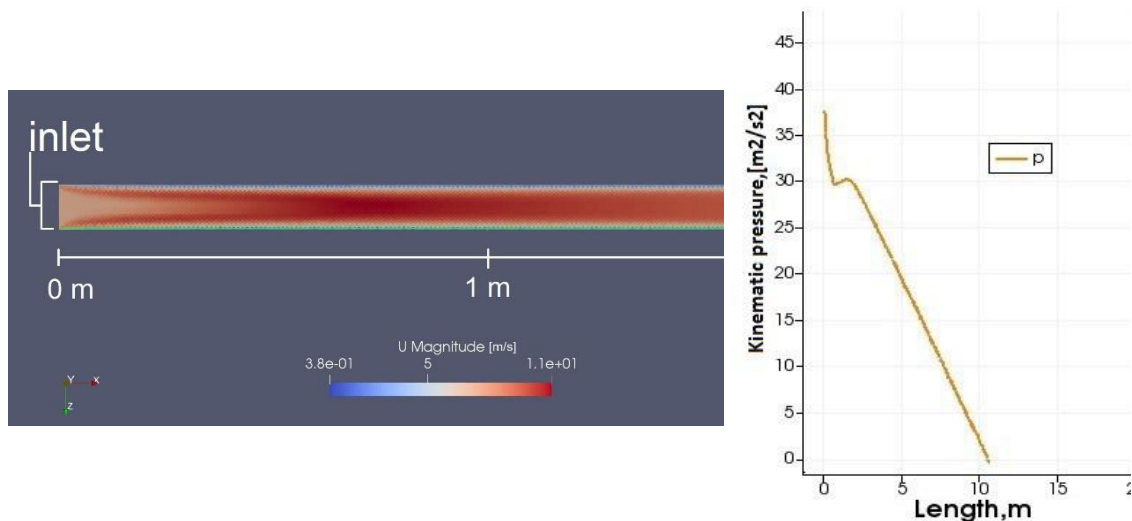


Figure 3.14. Side view of velocity distribution (left) and pressure values (right).

It can be seen from the fig.3.14 that turbulent flow develops at inlet in the first few meters. Pressure distribution along the pipe changes once turbulent flow has been developed. As was mentioned, this behavior of pressure drop and turbulent flow developing are because of flow rate boundary condition.

In order to assess the applicability of the OpenFOAM model it was proposed to consider 2D case. By doing so, it will be possible to create the better mesh and compare results to existing ones. If the results are similar the statement of OpenFOAM applicability will be proven.

However, to further clarify the affection of power conductors on pressure losses, tests will be carried out at NMPSE, details will be presented in the next chapter.

### 3.3 Dynamic Loads Analysis with DYNTUB Software.

The purpose of this analysis is to estimate the impact of dynamic loads during drilling caused by mass imbalance in DPC-127 which may lead to tool joints integrity and operability issues.

To solve this problem, universal DYNTUB software will be applied which is designed to simulate the dynamics of rigid bending drill string. The program will allow taking into account the impact of pipe body thickening due to tool joints on the longitudinal static and dynamic stability of BHA and DPC string (Tikhonov V.S. et al., 2014).

By applying the software, It is planned to obtain the values of such dynamic indicators of DPC working, as: vibration (frequency, [Hz]; maximum acceleration, [m/s<sup>2</sup>]), shocks (number of shocks per minute; maximum acceleration, [m/s<sup>2</sup>]; duration of impact, [ms]). With the help of the mentioned dynamic indicators, it will be possible to evaluate DPC elements interaction with wellbore.

Also, based on the analysis results, dependences of the change in drill string axis position related to well axis, contact force in time (at certain critical points) and depth (at certain points in time) will be constructed. The main parameter of the analysis is the contact force (in fact, overload) acting on power conductor, which makes it possible to assess the strength of its attachment to drill string.

The results of DYNTUB analysis will allow developing a standard for dynamic testing of DPC in real drilling conditions.

#### 3.3.1 Initial Data for Analysis

- 1) Wellbore profile - zenith and azimuth angle dependence on MD.
- 2) Wellbore design – parameters of the last casing and open wellbore.
- 3) DPC and BHA parameters. The mass-inertia properties of BHA elements with a length of less than 5 meters are included in the averaged equivalent assembly. More extended elements are considered as they are. Geometry of the protruding elements (centralizers, etc.) of BHA elements are considered as they are. The study considers one assembly only.
- 4) Drilling modes: RPM, WOB, mud density. In the calculation process, the influence of these parameters is analyzed in order to assess their impact and select optimal drilling mode.

*Table 3.13. Initial data for DYNTUBE.*

Parameters	Value	Unit
TVD	2030	m
MD	2727	m
Bit diameter	0,2207	m

Cavernous coefficient	1,1	-
Well diameter	0,231	m
Depth of previous casing	1080	m
Inner casing diameter	0,2292	m
Drill string for drilling with PMM		
DPC-127 hydraulic diameter	0,0852	m
Outer diameter of DPC-127	0,127	m
Outer tool joint diameter	0,168	m
Inner tool joint diameter	0,061	m
Length of DPC-127 section	2690	m
Pressure drop in PMM-178	0,5	MPa
BHA elements and their lengths		
Bit 220.7 - 0,2m;		
PMM-178 (motor and gearbox)- 15m;		
String Stabiliser - 1,9m;		
NMDC (non-magnetic drill collar)		
Pony 168 - 3,7m;		
6 3/4 Resistivitymetr DGR/EWR-P4 - 12,2m;		
6-3/4" TM Collar - 3,2m;		
DPC-127- 2690m;		
Mud properties and drilling modes		
WOB	3	tonn
RPM	200	rev/min
Flow rate	0,029	m <sup>3</sup> /s
Density	1150	$\frac{kg}{m^3}$
Plastic viscosity	0,015	$\frac{Pa \cdot s}{m^2}$
Yield strength	7	Pa

According to the calculation results, the axis change position dependences of drill string related to well axis and contact force in time (at certain critical points) and in depth (at certain points in time) will be constructed. The main parameter of the study is contact force (in fact, overload) acting on power conductors, which makes it possible to assess the strength of its attachment to the drill string wall.

The results of the DYNTUB program will allow developing a standard for dynamic testing of DPC in real drilling conditions.

### 3.4 Summary

Analytical calculations of pressure losses in DPC using WellPlan (Landmark), OpenFOAM software and standard techniques were considered in this chapter. Comparative hydraulic calculation of PMM application and traditional drilling methods showed significant increase in DPC-127 pressure losses, due to power conductors presence and reduced flow area in tool joints. It was proposed to manufacture DPC-140, which have superior hydraulic characteristics.

Calculations related to power conductors affection on pressure losses in DPC-127 showed that the equivalent diameter overestimates value of additional losses. For this reason, numerical modeling was performed in OpenFOAM software, according to the results of which additional losses accounted for 12,5 kPa (about 30%). However, the model created in OpenFOAM needs further improvements. To further clarify the pressure losses, the next chapter will consider tests at Neftekamsk Machine-Building Plant of special equipment.

## Chapter 4

### DPC Experimental Tests

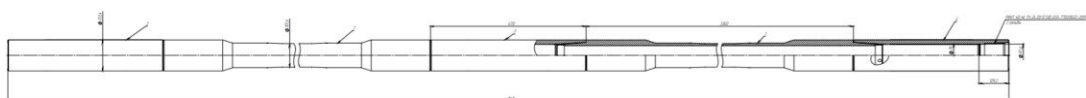
In this chapter experimental tests are presented allowing to clarify DPC design features affection on drilling process.

#### 4.1 Experimental Test of DPC Pressure Drop Estimation

Aim of test: (1) to estimate the pressure loss in drill pipes with power conductors (DPC) experimentally; (2) compare the results of the experiment with analytical analysis and modeling.

##### 4.1.1 Methodology of Experimental Tests

Objects of studies are two 4-meter DPC-127 and DPC-102 assemblies, made of 40HGMA (analog of A-4142HM) steel, with subs for connection to the test bench and excess pressure gauges installation (Fig. 1 and 2). Testing bench of Neftekamsk Machinery Plant of Special Equipment (NMPSE) is offered for testing. Testing bench is a part of drilling rig circulation system consisting of a container with drilling mud cleaning equipment installed, mud pumps, and closed circuit. The circulating agents are technical water and water with sand added (Fig. 3). To conduct the study, the assemblies with pressure sensors will be installed in horizontal part of the closed circuit, the scheme is shown in Fig. 4, where "S" is sealing element.



№	Исполнитель	Проверенный	Дата
1			
2			
3			
4			
5			
6			
7			
8			
9			
10			
11			
12			
13			
14			
15			
16			
17			
18			
19			
20			
21			
22			
23			
24			
25			
26			
27			
28			
29			
30			
31			
32			
33			
34			
35			
36			
37			
38			
39			
40			
41			
42			
43			
44			
45			
46			
47			
48			
49			
50			
51			
52			
53			
54			
55			
56			
57			
58			
59			
60			
61			
62			
63			
64			
65			
66			
67			
68			
69			
70			
71			
72			
73			
74			
75			
76			
77			
78			
79			
80			
81			
82			
83			
84			
85			
86			
87			
88			
89			
90			
91			
92			
93			
94			
95			
96			
97			
98			
99			
100			

Figure 4.1.DPC-102 assembly.

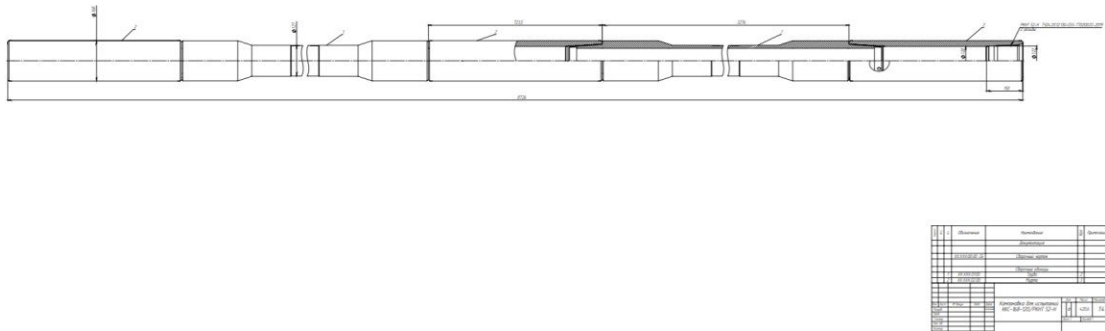


Figure 4.2.DPC-127 assembly.



Figure 4.3. Testing bench of NMPSE.

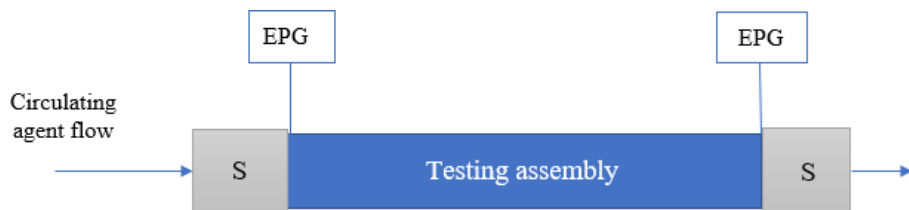


Figure 4.4. Installing scheme of the testing assemblies.

The tests will consist in pumping technical water and water with sand content simulating drilling mud through a closed circuit with pressure drop measurements at inlet and outlet. The two flow rates of each circulating agent will be considered.

Preliminary calculations are performed to evaluate the possible parameters of the experiment and select the appropriate excess pressure gauges.

## 4.1.2 Preliminary Hydraulic Analysis for Excess Pressure Gauges

### Selection and Experiment Planning – Initial Data

Hydraulic analysis will be performed for DPC-127 and DPCW-127 (with power conductors inside and without ones respectively) in order to select the appropriate pressure sensor applied in the tests (Leonov E., Simonyants S., 2014).

There will be two flow rates considered: the highest possible flow rate of mud pump ( $260 \frac{\text{m}^3}{\text{hr}}$ ) and 70% of the maximum flow rate ( $180 \frac{\text{m}^3}{\text{hr}}$ ). Also, two circulating agents are used: water and mud.

Table 4.1. Initial data.

Parameter	Value		Unit
Inner diameter of DPC-127	0,08552		m
Inner diameter of DPCW-127	0,105		m
Inner diameter of DPC-102	0,084		m
Length of DPC-127 (102)	4		m
Length of DPC-102 assembly	8,726		m
Length of DPC-127 assembly	8,614		m
Parameters of testing fluid			
	Water	Mud	
Density	1000	1150	$\frac{\text{kg}}{\text{m}^3}$
Plastic viscosity	0,01002	0,015	$\text{Pa} \cdot \text{s}$
Yield strength	0	7	$\text{Pa}$
Flow rate	260; 180		$\text{m}^3/\text{hr}$

First of all, it is necessary to calculate the critical value of the Reynold's number ( $Re_{cr}$ ):

$$Re_{cr} = 2100 + 7,3 \left( \frac{\rho d_i^2 \sigma}{\eta^2} \right)^{0,58} \quad (4.1)$$

Table 4.2. Critical Reynold's number.

Parameter	Value		Unit
$Re_{cr}$ of DPC-127	2100	12230	-
$Re_{cr}$ of DPCW-127	2100	14952	-
$Re_{cr}$ of DPC-102	2100	9997	-



After that, actual Reynold's number should be evaluated ( $Re_a$ ) for the given flow rates. Calculation formula and results are presented below:

$$Re_a = \frac{4\rho Q}{\pi\eta d_i} \quad (4.2)$$

Table 4.3. Actual Reynold's number.

Parameter	Value				Unit
Flow rate	260		180		$\frac{m^3}{hr}$
Testing fluids	Water	Mud	Water	Mud	-
$Re_a$ of DPC-127	107365	82478	74330	57100	-
$Re_a$ of DPCW-127	87446	67176	60540	46506	-
$Re_a$ of DPC-102	133071	102225	92126	70771	-

There is turbulent flow regime ( $Re_a > Re_{cr}$ ) in the pipes for all cases, and therefore the pressure loss in the pipe is determined by the Darcy-Weisbach formula:

$$\Delta P_p = \lambda_r \frac{8\rho Q^2}{\pi^2 d_i^5} l \quad (4.3)$$

where  $\lambda_r$  – hydraulic resistance coefficient.

Hydraulic resistance coefficients ( $\lambda_r$ ) is determined by:

$$\lambda_r = 0,1 \cdot \left( \frac{1,46K}{d_i} + \frac{100}{Re_a} \right)^{0,25} \quad (4.4)$$

where coefficient of roughness (K) is given by  $3 \cdot 10^{-4}$  m.

Table 4.4. Values of hydraulic resistance coefficients.

Parameter	Value				Unit
Flow rate	260		180		$\frac{m^3}{hr}$
Testing fluids	Water	Mud	Water	Mud	-
$\lambda_r$ of DPC-127	0,028	0,028	0,028	0,029	-
$\lambda_r$ of DPCW-127	0,027	0,027	0,028	0,028	-
$\lambda_r$ of DPC-102	0,029	0,029	0,029	0,030	-

It is also necessary to take into account pressure losses created by tool joints ( $\Delta P_{tj}$ ).

$$\Delta P_{tj} = \left[ \left( \frac{d_i}{d_{tj}} \right)^2 - 1 \right] \frac{16\rho Q^2}{\pi^2 d_i^4} \quad (4.5)$$

Table 4.5. Pressure losses created by tool joints.

Parameter	Value				Unit
Flow rate	260		180		$\frac{m^3}{hr}$
Testing fluids	Water	Mud	Water	Mud	
$\Delta P_{tj}$ of DPC-127	0,038	0,044	0,018	0,021	MPa
$\Delta P_{tj}$ of DPCW-127	0,004	0,004	0,002	0,002	MPa
$\Delta P_{tj}$ of DPC-102	0,008	0,009	0,004	0,004	MPa

Let us calculate pressure losses in the pipe body using Darcy-Weisbach formula.

Table 4.6. Pressure losses in the pipe body.

Parameter	Value				Unit
Flow rate	260		180		$\frac{m^3}{hr}$
Testing fluids	Water	Mud	Water	Mud	-
$\Delta P_p$ of DPC-127	0,219	0,255	0,107	0,125	MPa
$\Delta P_p$ of DPCW-127	0,076	0,089	0,037	0,044	MPa
$\Delta P_p$ of DPC-102	0,241	0,280	0,117	0,137	MPa

It is necessary to add up the pressure losses in pipe body and created by tool joints. The results are presented below.

Table 4.7. Results of analytical calculations.

Parameter	Value				Unit
Flow rate	260		180		$\frac{m^3}{hr}$
Testing fluids	Water	Mud	Water	Mud	-
$\Delta P_p$ of DPC-127	0,258	0,299	0,125	0,146	MPa
$\Delta P_p$ of DPCW-127	0,080	0,093	0,039	0,046	MPa
$\Delta P_p$ of DPC-102	0,249	0,289	0,121	0,141	MPa

The maximum values of pressure losses (0,299 MPa) can be observed in DPC-127 when mud circulating at the flow rate of  $260 \frac{m^3}{hr}$ . The minimal value of pressure losses is in DPCW-127 (0,039 MPa) when water circulating at the flow rate of  $180 \frac{m^3}{hr}$ .

Excess pressure gauge can be selected based on the approximate pressure range that expected during the test.

### 4.1.3 Excess Pressure Gauge Selection

To register pressure drop in the range from 0,039 MPa to 0,299 MPa (39kPa–299kPa), the application of PD100I excess pressure gauge manufactured by «Oven» (Russia, Dzerzhinsk) should be considered.

Compact pressure gauge represents the pressure transducer with membrane made of stainless steel and 4-20mA output signal.



*Figure 4.5. External view of excess pressure gauge (Teplopribor, 2022).*

Limits of permissible basic percentage error for sensors depend on sensor design. There are several possible designs with the following accuracy classes – 0,25 %; 0,5 %; 1,5 %. There are several measuring ranges available. Let us choose the range from 0 to 1000 kPa. In this case accuracy limits are as follows.

*Table 4.8. Accuracy limits of measuring range calculated.*

Accuracy limits, %	Accuracy limit of measuring range, kPa
$\pm 0,25$	$\pm 2,5$
$\pm 0,5$	$\pm 5$
$\pm 1,5$	$\pm 15$

It can be seen that minimal possible accuracy limit is  $\pm 2,5$  kPa. This is appropriate value of accuracy for the upcoming test.

Some types of pressure sensors from other manufacturers have more precise capabilities, for example, differential pressure transducer EMIS-BAR model 143 manufactured by «Emis» (Russia, Chelyabinsk) has accuracy limits accounting for 0,4 kPa for the same accuracy limit which has been proposed (EMIS, 2022). However, the manufacturing process of this pressure transducer would take about two months, so PD100I was purchased, which was available in storage facilities of "Oven" manufacturer.

#### 4.1.4 Test Plan

Below is the plan for the preparation and testing of drill pipes with power conductors at NMPSE testing bench.

*Table 4.9. Test plan.*

Work stage	Company or person in-charge
Drawings development and the assemblies manufacturing	Novobur company
The assemblies make-up process (DPC-127 и DPC-102)	Novobur company
Excess pressure gauges purchasing and checking	Novobur company
Loading, transportation and unloading of assemblies at NMPSE (Russia, Neftekamsk)	Novobur company - NMPSE
Mounting DPC-127 assembly and pressure gauges into the testing bench	Sherbakov.A.I. NMPSE
Circulating of technological agents at $180 \frac{m^3}{hr}$ flow rate within 10 minutes with registering pressure gauges readings	Sherbakov.A.I. NMPSE
Circulating of technological agents at $260 \frac{m^3}{hr}$ flow rate within 10 minutes with registering pressure gauges readings; Stop of circulation	Sherbakov.A.I. NMPSE
Demounting of DPC-127 assembly and the pressure gauges	Sherbakov.A.I. NMPSE
Mounting DPC-102 assembly and pressure gauges into the testing bench	Sherbakov.A.I. NMPSE
Circulating of technological agents at $180 \frac{m^3}{hr}$ flow rate within 10 minutes with registering pressure gauges readings	Sherbakov.A.I. NMPSE
Circulating of technological agents at $260 \frac{m^3}{hr}$ flow rate within 10 minutes with registering pressure gauges readings; Stop of circulation	Sherbakov.A.I. NMPSE
Endurance test of DPC-102 assembly within 200 hours	NMPSE
Demounting of DPC-102 assembly and mounting of DPC-127 one; Endurance test within 200 hours	NMPSE
Demounting of DPC-102 assembly; Assemblies loading and their transportation to Perm city	NMPSE

Due to the financial difficulties in Novobur and unpredicted delays in assemblies manufacturing, the test conduction date are clarified.

## 4.2 DPC Bench Test on Novobur Vibrostand.

To assess dynamic loads imitating field conditions, vibrostand of Novobur LLC will be applied for DPC testing. Before starting the tests, it is necessary to have the test standard, which is planned to be obtained from the results of DUNTUB software. Brief description of the vibrostand is given below and a possible test program is proposed, developed on the literature review basis of dynamic loads in drill string and malfunctions that may occur during drilling with DPC.

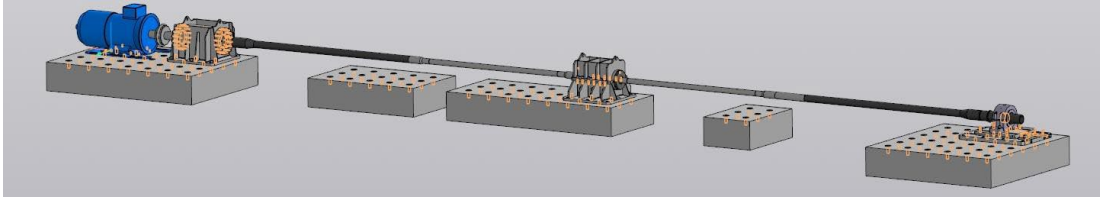


*Figure 4.6. Vibrostand of Novobur LLC for dynamic testing (Perelman O.M. et al., 2021).*

The vibrostand is designed for testing electric drill assemblies of various modifications and designs in conditions close to field ones. Testing assembly is exposed to vibration at acceleration up to 30g during testing. A possible DPC test program on the vibrostand is proposed below.

### 4.2.1 Test Program

The DPC test program on the vibrostand should be focused on establishing such drilling parameters (axial load and rotation frequency), at which damage to DPC elements, in particular, cable sections, may occur. Vibration and shocks occurring during the testing process may provoke the power conductors breakdown, therefore it is necessary to determine rotation frequency range of assembly and axial load on it, at which this problem occurs. The following test program is proposed.

*Table 4.10. Dynamic test program.*

Axial load on testing assembly, tons	Rotation frequency of assembly, RPM
2	20;40;60;80;100;120
4	20;40;60;80;100;120
6	20;40;60;80;100;120
8	20;40;60;80;100;120
10	20;40;60;80;100;120
12	20;40;60;80;100;120
14	20;40;60;80;100;120

The duration of the tests at each rotation frequency should be at least one minute. After examining each of the frequencies, it is necessary to check DPC integrity and cable sections out (for example, by checking the assembly current conductivity).

If DPC integrity damage are detected, tests should be immediately suspended and drilling parameters that led to the damage should be recorded. Next, it is necessary to clarify the threshold value of the frequency led to the damage. For example, if the breakdown occurred at axial load of 10 tons and frequency of 100 RPM, then it is necessary to examine the threshold value in the range of 80-100 RPM. When switching to next axial load value, the breakdown may occur in different range of the frequency values. At the end of the test, it will be possible to obtain the optimal area of DPC operation, in which there will be no damages of design integrity.





# Chapter 5

## Conclusion

### 5.1 Summary

The master thesis presented the experience of previous generation electric drilling complex application. A new electric drilling complex was considered, which is being developed by Novobur LLC and has prospects to make a technological breakthrough in the field of deep, multilateral, complex profiles, ERD wells. One of the key elements of this complex is drill pipes with power conductors, the design features of which require analysis of the hydraulic program and dynamic loads occurring during drilling.

Application of equivalent diameter concept in comparative hydraulic analysis shows the following results: the pressure loss when using PMM (DPC-127) is about 4% higher compared to PDM, and difference between RSS and PMM (DPC-127) is about 45,6%. These results indicate very significant increases in pressure losses due to the presence of cable sections, therefore, it is proposed to create DPC-140 with superior hydraulic characteristics when drilling wells of 210-220 mm.

Analytical methods for taking into account the influence of the cable show an increase in pressure losses by more than 30 kPa for one DPC pipe when compared with the case when there are no power conductors. This increase in pressure is too large if the dimensions of the cable sections are taken into account. Numerical modeling in OpenFOAM shows the more reliable results of cable accounting, pressure losses increase by about 12,5 kPa. However, the model created in this program may overestimate the pressure loss, as can be seen from the case of considering DPCW without cable inside. Nevertheless, this program provides a better assessment of the effect of turbulence and non-Newtonian flow models on pressure losses. In order to judge the applicability of a particular method of power conductors accounting inside DPC, experimental studies should be conducted using the stand of the Neftekamsk Machine-

Building Plant of special Equipment. The plan and methodology of upcoming tests were presented.

In the master's thesis, it was noted that cable sections in DPC-127 may create additional dynamic loads that can affect the integrity and operability of DPC. For this reason, it is proposed to use DYNTUB software with the subsequent development of a test method on the vibrostand of Novobur LLC with real drilling conditions simulation.

Electric drilling technology has advantages over traditional well construction technologies, which can ensure technical and economic performance growth of drilling. In order to achieve this, it is necessary to continue research and development to identify DPC operation features.

## **5.2 Evaluation**

On the one hand, to completely evaluate DPC operational features (dynamic loads and hydraulic losses) it is needed to conduct experimental studies, but they have not been conducted because of some delays and financial difficulties in Novobur LLC.

On the other hand, comparative hydraulic losses analysis between PMM and conventional methods of drilling application were presented. It should be noted that the aim of that analysis is to estimate possible hydraulic losses since the methodic applied was not accurate enough. Apart from it, OpenFOAM simulation of pressure losses was considered which showed more adequate affection of power conductors on pressure drop in DPC. However, OpenFOAM model has to be improved. Finally, test plan on NMPSE was developed and initial data to estimate dynamic loads in DYNTUB was demonstrated.

## **5.3 Future Work**

Further investigation of DPC exploitation features is planned including experimental test on NMPSE and dynamic loads estimation on vibrostand of Novobur LLC. Additionally, OpenFOAM model improvement will be completed as well as DYNTUB results analyzing.



## References

- Abyzbayev, B. I., Baibakov, N. K., Baidyuk, B. V., Gelfgat, Y. A., & Gelfgat, M. Y. (1997). Electrodrilling: Past Experience and Present Opportunities. *SPE Annual Technical Conference and Exhibition*.
- Altshul A., 1982. Hydraulic resistances. 2st ed. Moscow: Nedra. pp.96-98.
- CFD Direct. 2022. OpenFOAM v4 User Guide: 7.3 Transport/rheology models. [online] Available at: <<https://cfd.direct/openfoam/user-guide/v4-transport-rheology>> [Accessed 3 May 2022].
- Dareing D. W. (1984). Guidelines for controlling drill string vibrations. *Journal of Energy Resources Technology*.
- Dong, G. and Chen, P. (2016). A Review of the Evaluation, Control, and Application Technologies for Drill String Vibrations and Shocks in Oil and Gas Well. *Hindawi Publishing Corporation, Shock and Vibration*.
- Dykstra M. W., Chen D. C.-K., Warren T. M., Zannoni S. A. Experimental evaluations of drill bit and drill string dynamics. (1994). *SPE Annual Technical Conference & Exhibition*.
- EMIS. 2022. Pressure sensors 4-20 mA. [online] Available at: <<https://emis-kip.ru/ru/prod/davlenie/>> [Accessed 12 May 2022].
- Fomenko F.N, 1968. Electrodrills for oil and gas wells drilling. 1st ed. Moscow: Gostovtehzdat, pp.100-130.
- Fomenko F.N, 1974. Wells drilling by electrodrill. 1st ed. Moscow: Nedra, pp.53-95.
- Gelfgat, Y., Gelfgat, M. and Lopatin, Y. (2003). Advanced drilling solution, Lessons from the FSU. 1st ed. Tulsa: PennWell Corporation, pp.172-190.
- Hpc-education.ru. OpenFOAM lectures. 2022. [online] Available at: <[http://hpc-education.ru/files/lectures/2011/avetisyan/avetisyan\\_2011\\_slides10.pdf](http://hpc-education.ru/files/lectures/2011/avetisyan/avetisyan_2011_slides10.pdf)> [Accessed 3 June 2022].
- Jan A. Aasen and Bernt S. Aadnoy. Buckling model revisited. (2002). *IADC/SPE Asia Pacific Drilling Technology*.

- Javanmardi K. and Gaspard D. T. (1992). Application of soft-torque rotary table in mobile bay. *IADC/SPE Drilling Conference*.
- Leonov E. and Simonyants S., 2014. Deepening well technological process improving. 1st ed. Moscow: Publishing Center of I.M. Gubkin University of Oil and Gas, pp.130-155.
- Mitchell, R.F. (2000). Lateral Buckling of Pipe with Connectors in Horizontal Wells. *IADC/SPE Drilling Conference*.
- Perelman O.M., Fadeikin A.S., Gelfgat M.Ya., Geraskin A.S., Emirov Z.A. (2021). Prospects of electric drilling for the development of well construction technologies. 2021 SPE Russian Petroleum Technology Conference.
- Simonyants, S., 2018. Drilling of wells with hydraulic downhole motors. 1st ed. Moscow: Publishing Center of I.M. Gubkin University of Oil and Gas, pp.130-155.
- Menand S., Farrag M., DrillScan. (2019). How Does Buckling Impact Drilling & Completion Performance in Unconventional Wells. *AADE National Technical Conference and Exhibition*.
- Teplopribor.pro-solution.ru. 2022. [online] Available at: <<https://teplpribor.pro-solution.ru/wp-content/uploads/2019/09/%D0%A0%D0%AD-CROCUS-L-2019.06.19.pdf?ysclid=13yk8tjqu5>> [Accessed 1 June 2022].
- Tikhonov V.S., Safronov A.I., Valiullin H.R., Bukashkina O.S. et al. (2014). Development of Universal Application for Drillstring Dynamics Simulation. 2014 SPE Russian Petroleum Technology Conference.
- Tikhonov V.S., Valiullin H.R., Ring L. et al. (2012). Numerical simulation of well trajectory while drilling isotropic and anisotropic formations. *ASME Conference on Engineering Systems Design and Analysis ESDA*.



## List of Figures

Figure 2.1. Electrical three-line drill pipe design (Fomenko F.N., 1974) .....	14
Figure 2.2. Electrodrilling system of 60-70s generation set-up (Abyzbaev B.I. et al., 2003) ...	16
Figure 2.3. Drill pipe with two-line current lead (Abyzbaev B.I. et al., 2003) .....	17
Figure 2.4. Submersible electromagnetic contactor (Fomenko F.N., 1968) .....	17
Figure 2.5. R&D conducted by Novobur LLC (Perelman O.M. et al., 2021) .....	20
Figure 2.6. DPC-102 (upper figure) and DPC-127 (lower figure) (Novobur LLC) .....	21
Figure 2.7. Drill string vibration types .....	26
Figure 2.8. Modern tool for drill string vibration detection (Dong, G. and Chen, P., 2016) .....	27
Figure 2.9. Estimation criteria of drill string vibration (Dykstra M.W. et al., 1984) .....	28
Figure 2.10. Optimum zone concept for PDC bits (Javanmardi K. Gaspard D. T, 1982.) .....	28
Figure 2.11. Typical V&S absorber (Dong, G. and Chen, P., 2016) .....	29
Figure 2.12. Soft torque rotation system configuration (Javanmardi K., Gaspard D. T, 1982). .....	30
Figure 2.13. Semiactive vibration damper (Dong, G. and Chen, P., 2016) .....	31
Figure 2.14. DYNTUB timestep (Tikhonov V.S. et al., 2012) .....	32
Figure 2.15. Critical force for helical buckling. (Menand S. et al., 2019) .....	33
Figure 2.16. Typical buckling behavior in unconventional well – Bending Stress and Contact Forces (vectors). (Menand S. et al, 2019) .....	34
Figure 2.17. Tension/Compression along the drill string while drilling (Menand S. et al, 2019). .....	34
Figure 2.18. Cross-section of DPC-127 (inner diameter-105mm) (Novobur LLC) .....	36
Figure 3.1. Well design (Novobur LLC) .....	40
Figure 3.2. Pressure distribution along the wellbore .....	41
Figure 3.3. Interrelation of total pressure losses (standard methodic results are shaded) .....	42
Figure 3.4. Pressure distribution along the wellbore .....	44
Figure 3.5. Interrelation of total pressure losses (standard methodic results are shaded) .....	45
Figure 3.6. Navier-Stokes equations for an incompressible fluid (Hpc-educaiton, 2011) .....	47
Figure 3.7. Model of DPCW and names of its faces .....	49
Figure 3.8. The other side of DPCW (where “cut” face is located) .....	49
Figure 3.9. left) DPC geometry and right) DPC after meshing .....	50
Figure 3.10. left) DPCW geometry and right) DPCW after meshing .....	50
Figure 3.11. Residuals for DPCW case .....	54
Figure 3.12. Results of analytical and numerical pressure losses analysis .....	55
Figure 3.13. Velocity distribution at outlet of DPCW .....	56
Figure 4.1. DPC-102 assembly. ....	61
Figure 4.2. DPC-127 assembly. ....	61
Figure 4.3. Testing bench of NMPSE .....	61
Figure 4.4. Installing scheme of the testing assemblies .....	61
Table 4.5. Pressure losses created by tool joints .....	64
Figure 4.5. External view of excess pressure gauge (Teplopribor, 2022) .....	66
Figure 4.6. Vibrostand of Novobur LLC for dynamic testing (Perelman O.M. et al., 2021) .....	68

## List of Tables

Table 3.1. Initial data for hydraulic analysis of intermediate casing with a diameter of 178 mm .....	39
Table 3.2. Pressure losses while drilling for 178 mm intermediate casing (* - Given mud; results in brackets are obtained by standard methodic).....	41
Table 3.3. Initial data for 114 mm liner drilling.....	43
Table 3.4. Pressure losses while drilling for 114 mm liner (* - Given mud; results in brackets are obtained by standard methodic) .....	44
Table 3.5. Initial data for analytical calculations and simulation.....	48
Table 3.6. The results of analytical calculations .....	49
Table 3.7. Mesh parameter for DPC and DPC.....	50
Table 3.8. Mesh problems.....	50
Table 3.9. Boundary and internal field conditions .....	52
Table 3.10. Transport model, turbulence and case control properties .....	53
Table 3.11. Results of simulation.....	53
Table 3.12. Result comparison.....	54
Table 3.13. Initial data for DYN TUBE.....	57
Table 4.1. Initial data .....	62
Table 4.2. Critical Reynold's number.....	62
Table 4.3. Actual Reynold's number .....	63
Table 4.4. Values of hydraulic resistance coefficients.....	64
Table 4.5. Pressure losses created by tool joints .....	64
Table 4.6. Pressure losses in the pipe body.....	65
Table 4.7. Results of analytical calculations.....	65
Table 4.8. Accuracy limits of measuring range calculated. ....	66
Table 4.9. Test plan.....	67
Table 4.10. Dynamic test program.....	69



# Nomenclature

$m$	mass	[kg]
$E$	Young's modulus	[Pa]
$I$	Initial turbulence intensity	[-]
$k$	turbulent kinetic energy	[m <sup>2</sup> /s <sup>2</sup> ]
$\omega$	Specific dissipation	[1/s]
$L$	turbulent length scale	[m]
$Q$	flow rate	[m <sup>3</sup> /s]
$K$	coefficient of roughness	[mm]
$\mu$	viscosity	[Pa·s]
$Re$	Reynold's number	[-]
$n$	flow index	[-]
$K'$	consistency index	[Pa·s <sup>n</sup> ]
$l$	length	[m]
$\rho$	density	[kg/m <sup>3</sup> ]
$\eta$	plastic viscosity	[Pa·s]
$\lambda_r$	hydraulic resistance	[-]
$\Delta P$	pressure drop	[Pa]
$U$	mean velocity	[m/s]

# Abbreviations

BHA	Bottomhole Assembly
DP	Drill Pipe
DPC	Drill Pipe with Power Conductors
DPCW	Drill Pipe without Power Conductors
EDC	Electrical Drilling Complex
EDM	Electric Downhole Motor
ERD	Extended Reach Drilling
MWD	Measurements While Drilling
NMPSE	Neftekamsk Machinery Plant of Special Equipment
OBM	Oil Based Mud
PDC	Polycrystalline Diamond Compact Bits
PDM	Positive Displacement Motor
PMM	Permanent Magnet Motor
ROP	Rate of Penetration
RPM	Revolutions per Minute
RSS	Rotary Steerable System
TOB	Torque on Bit
WBM	Water Based Mud
WOB	Weight on Bit